DEVELOPMENT AND VALIDATION OF A FINITE ELEMENT MODEL OF A TRANSPORT AIRCRAFT SEAT UNDER PART 25.562 DYNAMIC TEST CONDITIONS

A Thesis By

Nilesh E. Dhole

Bachelor of Engineering, University of Pune, 2006

Submitted to Department of Mechanical Engineering
and the Faculty of Graduate School of
Wichita State University
in partial fulfillment of
the requirements for the degree of
Master of Science

May 2010

DEVELOPMENT AND VALIDATION OF A FINITE ELEMENT MODEL OF A TRANSPORT AIRCRAFT SEAT UNDER PART 25.562 DYNAMIC TEST CONDITIONS

The following faculty members have examined the final copy of this thesis for the form and content, and recommend that it be accepted in partial fulfillment of the requirement for the degree of Master of Science with a major in Mechanical Engineering.

_____

Hamid Lankarani, Committee Chair

_____

Gerardo Olivares, Committee Member

_____

George Talia, Committee Member

DEDICATION

To my Parents **Kalavati** and **Ekanath Dhole**,

Brother **Aviansh** and Sister-in-law **Pooja**

for their continuous encouragement, love and support

And

To all my **Friends**

ACKNOWLEDGEMENT

I express my sincere gratitude to my advisor, Dr. Hamid Lankarani, Professor of Mechanical Engineering, for his support, encouragement, and timely guidance throughout my graduation studies at Wichita State University. His continuous encouragement and support made possible the successful completion of this thesis.

I also thank Dr. Gerardo Olivares, Technical Director Computational Mechanics and Crash Dynamics Laboratory from the National Institute of Aviation Research (NIAR) for giving me the opportunity to work on this research project, and for his invaluable advice, continuous guidance and support while working in the Computational Mechanics Laboratory at NIAR.

I express my gratitude to Dr. George Talia, Chair Mechanical Engineering Department for being my thesis committee member and suggestions on my thesis.

I would like to extend special thanks to Mr. Vikas Yadav, Senior Research Engineer from National Institute of Aviation Research (NIAR) for all technical discussions and suggestions. I also would like to thank Richard DeWeese and David Moorcroft from CAMI crash dynamics laboratory for providing me a sample of the aircraft seat test article and dynamic sled test data.

I am indebted to all my colleagues from NIAR Computational Mechanics Laboratory for their continual help during my research project.

Lastly, I am grateful to my parents, brother and sister-in-law for their unconditional support and encouragement throughout my graduation studies.

ABSTRACT

Computer simulations are becoming a crash analysis method that will enable more effective, efficient and verifiable crashworthy aircraft design. Greater use of computer simulation is being employed to understand wide range of crashworthiness related areas. Efforts are also being made to reduce the certification testing cost of aircraft seats and improve the occupant safety through computer simulation techniques.

The objective of this thesis were to generate a finite element model of a typical passenger aircraft seat with the explicit FE code LS-DYNA to validate the simulation model against test data, then to use it for parametric case studies. Additional emphasis was put on following the rules and regulations described in AC 20-146 for computer modeling techniques.

Thesis report includes validation of finite element of a typical aircraft seat generated using the FE explicit code LS-DYNA. Full scale dynamic tests were conducted as per 14 CFR PART 25-562. Kinematic frames comparison and profile matching using Sprague and Geers method was used as a validation tools. The model was then used for a parametric study to investigate the response of the seat with different seat belt and cushion.

TABLE OF CONTENTS

Chapter **Page**

TABLE OF CONTENTS (Continued)

Chapter **Page**

TABLE OF CONTENTS (Continued)

Chapter **Page**

LIST OF TABLES

Table **Page**

LIST OF FIGURES

Figure **Page**

LIST OF FIGURES (Continued)

Figure **Page**

LIST OF FIGURES (Continued)

Figure **Page**

LIST OF FIGURES (Continued)

Figure **Page**

LIST OF ABBREVIATIONS

AC	Advisory Circular
ATD	Anthropomorphic Test Dummy
CAE	Computer Aided Engineering
CAMI	Civil Aero Medical Institute
CFC	Channel Frequency Class
CFR	Code Federal Regulation
FAA	Federal Aviation Administration
FE	Finite Element
FTSS	First Technology Safety Services
GASP	General Aviation Safety Panel
HIC	Head Injury Criteria
NIAR	National Institute for Aviation Research
TSO	Technical Standard Order
WSU	Wichita State University

CHAPTER 1

INTRODUCTION

Full scale dynamic certification testing of aircraft seats is very expensive and time consuming process. One reliable solution to reduce certification cost and time is to produce better seat design by predicting the dynamic behavior of seating system, using computer aided finite element modeling techniques.

Engineering problems are nothing but the mathematical models of physical systems. Mathematical models are represented by differential equations with a set of corresponding initial and boundary conditions. These differential equations are derived by applying the fundamental laws and principles of nature to a system or a control volume. Governing equations of these mathematical models represent balance of mass, force, or energy.

Mathematical model for simple problems with columns or trusses can be very easily derived to get the exact solution. However there are many practical engineering problems such as high speed impact test of aircraft seats, for which we cannot obtain exact solutions that easily. This inability to obtain an exact solution may be attributed to either the complex nature of governing differential equations or the difficulties that arise from dealing with the boundary and initial conditions. To deal with such problems, we take help of numerical methods.

Advances in computer software and hardware have made it possible to analyze complex systems by numerical simulation. With the availability of low cost, fast computers, it is possible to tackle large crash impact problems. As a result, FEA techniques have become a well-established design tool for predicting dynamic events in the aircraft seat industry.

1.1 Motivation

Today's aircraft industry is trying to solve the primary causes of severe injury or death in survivable aircraft crashes through advancing crashworthiness technology. Computer simulations are becoming a crash analysis method that will enable more effective, efficient and verifiable crashworthy aircraft design. Greater use of computer simulation is being employed to understand wide range of crashworthiness related areas. For example the effect of size, shape and pressure of airbag on occupant injury is being analyzed, use of airbags to reduce helicopter ditching problems is being understood and structural damage due to different bird strike scenarios is being determined.

Efforts are also being made to reduce the certification testing cost of aircraft seats and improve the occupant safety through computer simulation techniques. Advances in computer software and hardware have made it possible to analyze complex systems by numerical simulation. With the availability of low cost, fast computers, it is possible to tackle large crash impact problems. As a result, FEA techniques have become a well-established design tool for predicting dynamic events in the aircraft seat industry. FAA and aircraft industries are working together to make FEA a certification tool, known as Certification By Analysis or CBA.

1.2 Objective

Objective of this thesis was to generate a finite element model of a typical passenger aircraft seat with the explicit FE code LS-DYNA, validate the simulation model against test data and then use it for parametric case studies. Additional emphasis was put on following the rules and regulations described by AC 20-146 for computer modeling techniques.

1.3 Literature Review

Soltis and Olcott [1] have reviewed the development of dynamic performance standards which were incorporated into Part 23 of the Federal Aviation Regulations and were based on a comprehensive analysis of full scale aircraft impact tests, general aviation aircraft accident data analysis and a dynamic test program of general aviation seats. Before 1970's aircraft seats were designed with only static strength requirements. In 1970's FAA and NASA conducted a test series of 21 full scale impact tests to generate a substantial database regarding the crash behavior and occupant characteristics of small general aviation aircraft. The General Aviation Safety Panel (GASP) was formed to conduct the crashworthiness research and to develop recommended crash dynamic design standards. GASP conducted a thorough research on pulse shape, pulse duration and survivable accident limits. They also proposed pass/fail criteria by defining performance criteria that directly related selected parameters measured during the dynamic test to injury criteria that is based on human impact injury limits. These performance criteria evaluate the occupant /seat protection system's potential for preventing or minimizing injuries from both primary and secondary impacts. In early 1983 GASP submitted its report to FAA and then it was incorporated into Part 23 of FAR. Dynamic tests standards suggested by GASP provide a more representative evaluation of the occupant/seat/restraint system interaction, yield data for impact injury analysis and prove data to assess the function of an energy absorber system where provided.

AGATE report no. C-GEN-341-1 [2] provides the guidance for demonstrating compliance with FAR part 23-562 by computer modeling analysis techniques. It provides sufficient details to develop the seat or occupant model that can be used for design and certification and the validation criteria for computer model. It explains AC 20-146 along with the good practice for

computer modeling documentation procedure. It also focuses on the testing of the seat and installation procedures. Different techniques for contact modeling, constraint modeling and belt modeling are also explained for Multi-body and Finite Element methods. A brief description of different types of elements used in Multi-body and FE modeling process is given along with details on available occupant models. Selection of appropriate material models for metallic parts, composites and seat foam cushions is explained for FE code Dytran.

Adams, Lankarani and Nick [3] showed the capacity of computer models as a new low cost and effective evaluation method for crashworthiness of aircraft seats. First approach was to develop the FE model of the seat for a FE code LS-DYNA to analyze the dynamic behavior of the seat under direct impact. In the second approach Multi-Body solver MADYMO is used to study the kinematic behavior of the occupant. Hybrid II 50^{th} percentile ATD was used to simulate Test I and II conditions of FAR part 23-562. Finally to increase the simulation accuracy third approach was used with coupling of FE and Multi-body techniques. Paper concludes with computer models as simple, fast and effective seat design tool which can predict dynamic responses of the seat when subjected to crash event.

Christian and Axel [4] investigated the applicability of dynamic simulations with Ls-Dyna for aircraft seat applications. It discusses about the old and new rules of the seat certification structural tests and injury criteria. Author gets some differences in simulations as compared to testing for Test II conditions and comes to conclusion that these differences are because he did not include the pre-stresses and deformations from implicit analysis to dynamic simulations. Author concludes that dynamic finite element simulation with Ls-Dyna is a suitable method in aircraft seat development to predict crash behavior.

The research conducted by Gabler, Bowen and Molnar [5] was objected to develop a finite element model of aircraft seat using Ls-Dyna computer code. In accordance with FAA passenger seat was chosen for modeling and testing. By the process of reverse engineering seat geometry has been created from dismantling actual seat. Seat drop testes were carried out by dropping the seat from different seat heights. The finite element model was used to simulate impact tests of the reference seat with an instrumented dummy at increasingly severe impact velocities. The resulting model was served as computational tool for future evaluation and development of energy absorbing seats for commuter category aircrafts.

Schoenbeck [6] discusses some of the emerging technologies in aircraft crashworthiness. Paper explains some of the differences in static and dynamic testing conditions and drawbacks of static testing. Author explains some of the details of a crash analysis tool known as KRASH. It was a hybrid code as to predict the overall response of structure it needs some crash response characteristics as input. This paper also focuses on hydrodynamic crash analysis using MSC/DYTRAN. Some of the differences between ground impact and water impact are also explained in this paper. Implementation of restraint airbag system using MADYMO is also discussed.

Lankarani and Bhonge [7] have suggested some strategies for finite element modeling of aircraft seats in this paper. The process of FE modeling of seats for the explicit dynamic code LS-DYNA has been described in detail along with a case study. According to author combination of shell and solid elements can be used to model structural components. The choice of elements depends on the geometry, cross section of component and how critical the component is. Author also suggests using dummy shell elements when combination of shell and solid elements is used. Bolt modeling is done using beam element and rigid spiders, but to get

accurate results author suggest to go for component level simulation with meshing of actual bolt. For nonstructural components like seat foams, author suggests to use fully integrated element formulation to get accurate results. Author also have discussed some of the topics like post processing, mass scaling, penetrations, energy balance and hourglass energy. Case study shows the results for FE model of seat for PART 25-562 Test II condition. Static deformation of pitch and roll were dynamically performed while actual pulse was acting. Results comparison of test and simulation was also shown.

CHAPTER 2

CRASHWORTHINESS REGULATIONS

2.1 Introduction

This chapter is a short review of the 14 CFR PART 25.562 and advisory circular 20-146. PART 25.562 [8] is the Aircraft Seat Crashworthiness Regulation for Transport Airplanes and used as guideline for certification testing. Dynamic tests standards suggested by PART 25.562 provide a more representative evaluation of the occupant/seat/restraint system interaction, yield data for impact injury analysis and prove data to assess the function of an energy absorber system where provided.

Dynamic Seat Certification by Analysis i.e. AC 20-146 [9] describes procedure for simulation when used as certification by analysis tool. Computer simulations are becoming a crash analysis method that will enable more effective, efficient and verifiable crashworthy aircraft design. Greater use of computer simulation is being employed to understand wide range of crashworthiness related areas. Efforts are also being made to reduce the certification testing cost of aircraft seats and improve the occupant safety through computer simulation techniques.

2.2 14 CFR PART 25.562

In this section, PART 25.562 i.e. Aircraft Seat Crashworthiness Regulation for Transport Airplanes is discussed. This document explains aircraft seat crashworthiness regulation and the pass/fail or performance criteria for Transport category airplanes. The basic information related to test conditions, acceleration pulse requirements and anthropomorphic test devices is elaborated.

2.2.1 Aircraft Seat Crashworthiness

Aircraft seats have traditionally been designed to comply with static strength requirement of 9g [10]. There were no occupant injury criteria involved in the regulations and not much importance was given to the seat energy attenuation. In the summer of 1982 GASP was formed on the request of FAA representing a board constituency from the general aviation community for the purpose of recommending regulatory or non regulatory means by which the FAA could increase general aviation safety [1]. In early May 1984 GASP submitted its report for enhanced crash tolerance for small, FAR Part 23 general aviation aircraft [1]. Dynamic tests standards suggested by GASP provide a more representative evaluation of the occupant/seat/restraint system interaction, yield data for impact injury analysis and prove data to assess the function of an energy absorber system where provided.

2.2.2 Aircraft Seat Crashworthiness Regulations

From the existing crash studies GASP established pass/fail performance criteria which evaluates the seat and restraint system's potential for preventing or minimizing injuries from primary impacts, secondary impacts and occupant skeleton loads. The aim was, passengers in fatal crash situation like emergency landing, can still able to free themselves independently and escape the aircraft having good chance to survive. Realistic dynamic performance standards for aircraft seats which emphasize occupant impact protection and which were based on comprehensive analysis of full-scale aircraft impact tests, parametrical studies using crash dynamics computer programs, accidental data analysis, and dynamic test programs of aircraft seats have been defined. These performance standards take the form of two dynamic test conditions [1] as explained in sections 2.2.3 and 2.2.4.

2.2.3 Test I Condition

This test determines the performance of the system in a test condition where the predominant impact force component is along the spinal column of the occupant in combination with a forward impact force component. This test evaluates the structural adequacy of the seat, critical pelvic/lumbar column forces, and permanent deformation of the structure under combined downward and forward impact loading. Setup for this test is shown in Figure 2-1.

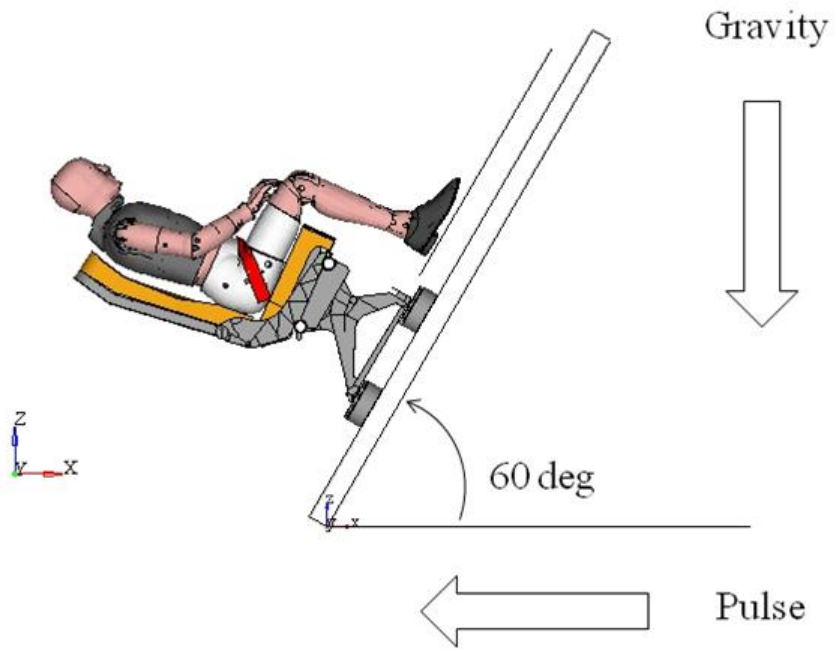

Figure 2-1 Test I simulation setup

2.2.4 Test II Condition

The purpose of this test is to determine the performance of a system in a test condition where the predominant impact force component is along the longitudinal axis of the airplane in combination with a lateral impact force component. This test evaluates the structural adequacy of the seat, and permanent deformation of the structure. It also evaluates behavior and loads of the pelvic restraint and, if applicable, of the upper torso restraint. The test may also yield data on

ATD head displacement, velocity, and acceleration time histories as well as the seat leg loads imposed on the seat tracks or attachment fittings. Simulation model setup for this test is shown in Figure 2-2.

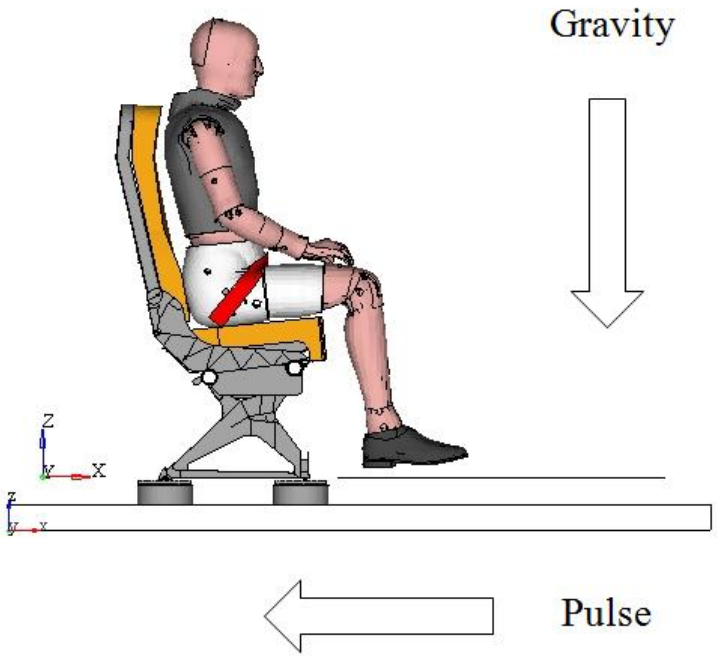

Figure 2-2 Test II simulation setup

This test requires simulating deformation between the seat and airplane floor by deforming the test fixture, prior to applying the dynamic impact conditions. The purpose is to demonstrate that the seat/restraint system will remain attached to the airframe and perform properly, even though the airplane and/or seat are deformed by the forces associated with a crash.

The floor deformation is achieved statically by pitching one leg in the structure and rolling the other one. 10^0 yaw is also applied on the test 2 condition. In both the test conditions,

Hybrid II, 50th percentile male ATDs' are used to evaluate the seat structure. Figure 2-3 shows details of test condition I and II for Aircraft type Part 25.

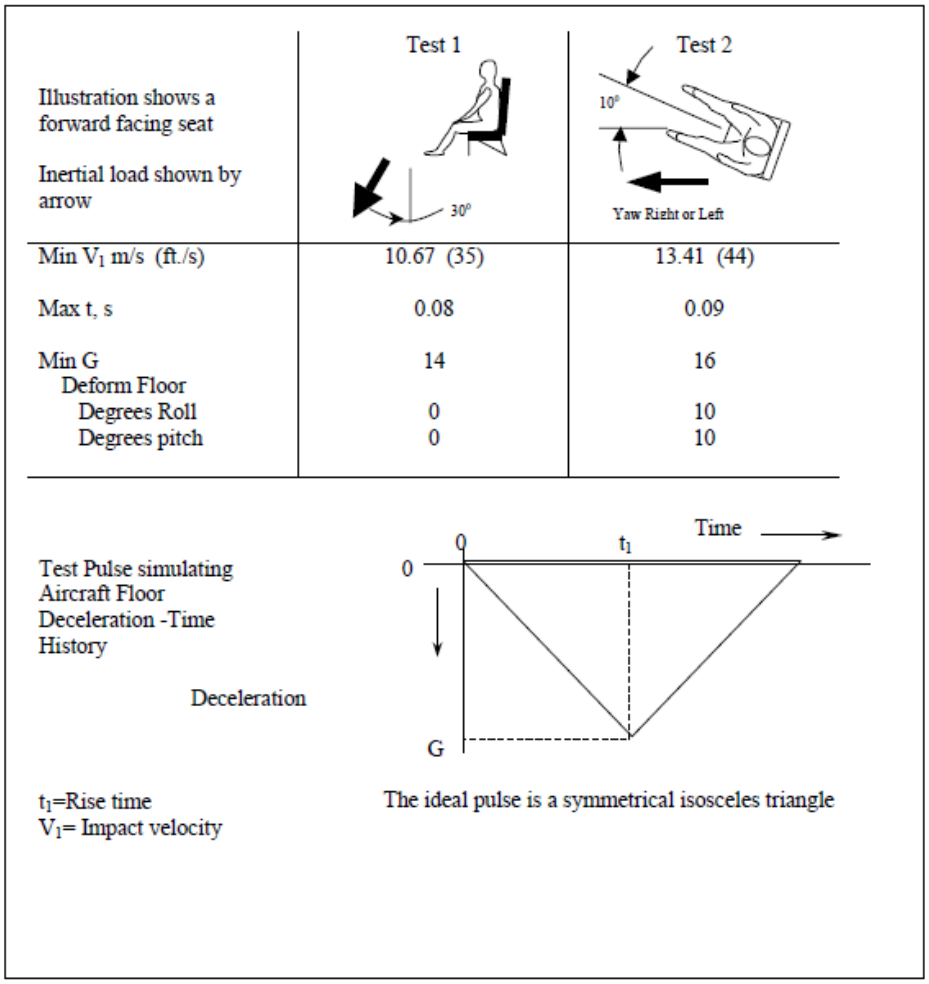

Figure 2-3 Seat/restraint system dynamic tests [8]

This AC also describes the pass/fail criteria or performance criteria to evaluate the structure or occupant's potential in preventing or minimizing the injuries caused due to the impact forces. These performance criteria's are summarized in section 2.2.5 and 2.2.6 in the form of occupant injury criteria and structural integrity.

2.2.5 Occupant Injury Criteria

- HIC is a measurement that insures the occupant will remain conscious following a survivable accident. In any circumstances if the occupant or the ATD's head is exposed to the impact with the interior features like monuments, seat structures, aircraft frame during the test, occupant HIC should not be exceeded 1000 or if the contact occurs, protection must be provided so that the head impact does not exceed the HIC of 1000.
- The maximum compressive load measured between the pelvis and the lumbar column of the ATD does not exceed 1,500 lbf (6.67 kN).
- In case of torso restraints are used, tension loads in individual straps do not exceed 1,750 lbs (7.78 kN).
- If dual straps are used for restraining the upper torso, the total strap tension load does not exceed 2,000 lbs (8.90 KN).
- The upper torso restraint straps remain on the ATD's shoulder during the entire test.
- The pelvic restraint remains on the ATD's pelvis during the entire test.
- Where leg contact with seat or seats, with monuments occurs, the axial compressive load in each femur does not exceed 2,250 lbs (10.0 kN).

2.2.6 Structural Integrity

- The seating system must remain attached to the test fixture at all points of attachment, the occupant restraint system must remain attached at all points of attachment. The primary load path must remain intact.
- Failures in any part of the primary load path, including the seat attachment to the track or restraint system attachment to the seat, will require a retest.

- Cracking of structural elements and the shearing or separation of rivets and minor delamination of composite panels is allowed, provided a continuous load path remains between the occupant and the seat attachments.
- Seat deformations must not yield to the extent that it would impede rapid evacuation of the occupants in the airplane. Seat permanent deformations such as seat-pan angle, seat backrest deformation must be in the quantitative limits is mentioned in Appendix 2 of AC

2.3 Advisory Circular 20-146

This section discusses the methodology of seat certification by analysis. It is the brief overview of the advisory circular 20-146. This chapter provides guidance on how to validate the computer model and under what conditions the model may be used in support of certification. This chapter also discusses the acceptable applications, limitations, validation processes, and minimum documentation requirements involved when substantiation by computer modeling is used to support a seat certification program.

2.3.1 Validation Criteria

This topic discusses different parameters validation criteria that need to be fulfilled as per the regulation of the application.

- Occupant Trajectory

Occupant trajectory is determined to evaluate the overall occupant movement envelop. Overall translational and rotational motion of the occupant is determined for head, pelvis and torso. Trajectory obtained from simulation should be compared to photometric data of actual test.

- Floor Reaction Loads

Structural response includes critical floor reaction loads and structural deflections of the seat. Validation of floor reactions should include only critical axial components and not all three axial components. As Floor loads evaluate a properly modeled load path of an occupant and seat system, these are important parameters of validation and should correlate within 10% to test data.

- Restraint Systems

Restraint system is a primary load path component and plays important role in keeping occupant attached to seat. For restraint system correlation within 10% is required to ensure correct load transfer.

- Head Injury Criteria (HIC)

1,000 units is the maximum allowable HIC limit. For head acceleration profile from simulation should correlate to test time history data. The allowable difference between test and simulation for validation is of 50 HIC units.

- Spine Load

1500 pounds of compressive load is allowable spine load. 10% of difference between peak spine load and time history plot of test and simulation is allowed.

- Femur Compressive Load

Femur compressive load has the allowable limit of 2250 pounds. Simulation data of femur compressive load should correlate within 10% to that of test data.

2.3.2 Description of Computer Model

This section spreads a light on a document that provides the analytical results and comparisons to test data when computer modeling is submitted as engineering data, known as the Validation and Analysis Report (VAR).

The VAR contains a detailed description of the computer model, including the input data. It must also include a discussion on the topics from the following sections

- Engineering Assumptions
- Finite Element Modeling of the Physical Structure
- Material Models
- Constraints or Boundary Conditions
- Load Application
- Occupant Simulation
- General Analysis Control Parameters

CHAPTER 3

DESCRIPTION OF FINITE ELEMENT MODEL

3.1 Introduction

This section contains a detailed description of the Finite Element (FE) or computer model. Structure used to write this chapter was as per the guidelines of AC 20-146 for documentation. This section includes discussion on the topics like unit system, assumptions used for FE model, material models used, constraints applied in model etc. in the following sections.

3.2 Units

Different kind of unit systems can be used for modeling until and unless the units are consistent with each other. The unit system used for FE model was as follows

Length : millimeter

Mass : ton

Time : second

Force : newton

Stress : mega pascal

3.3 Engineering Assumptions

Development of FE model always comes with certain engineering assumptions because modeler has to maintain balance between CPU cost and modeling of small features of geometry. Small features like surface fillets with small radius or very small holes have to remove while meshing so as to maintain computational time step. Some of the components which does not include in primary load path or some plastic parts which does not contribute to stiffness of the

structure such as life vest, video monitor or tray were omitted from FE model. Ballast weights were used to compensate the weight of these removed components and mass of the FE model was maintained same as test article.

3.4 Geometrical and Finite Element Modeling Process

The most representative technique to model structural objects is to use the finite element method. FE models are generated to obtain detailed response of structures and to determine structural failure. Finite element models are more difficult to generate than multi-body models, however, FE models are more practical because they predict realistic structural response and offer the capability to output stresses, strains and internal loads. They can also be utilized to substantiate structural designs. This section describes the geometrical and finite element modeling process.

3.4.1 Geometrical Modeling Process

Since the seat model used for this thesis was old design and no cad data was available for seat design. So this research started with geometrical modeling of the seat by the process of reverse engineering; meaning cad data for the seat was generated from actual seat. To generate the geometrical cad data seat was taken apart then each and every part was measured accurately or digitized. CATIA V5 R18 was used to generate geometrical model of the seat. Even the non metallic parts like seat cushions were modeled using the same procedure of reverse engineering. Figure 3-1 shows the comparison of some of the actual structural components and their 3D cad geometry.

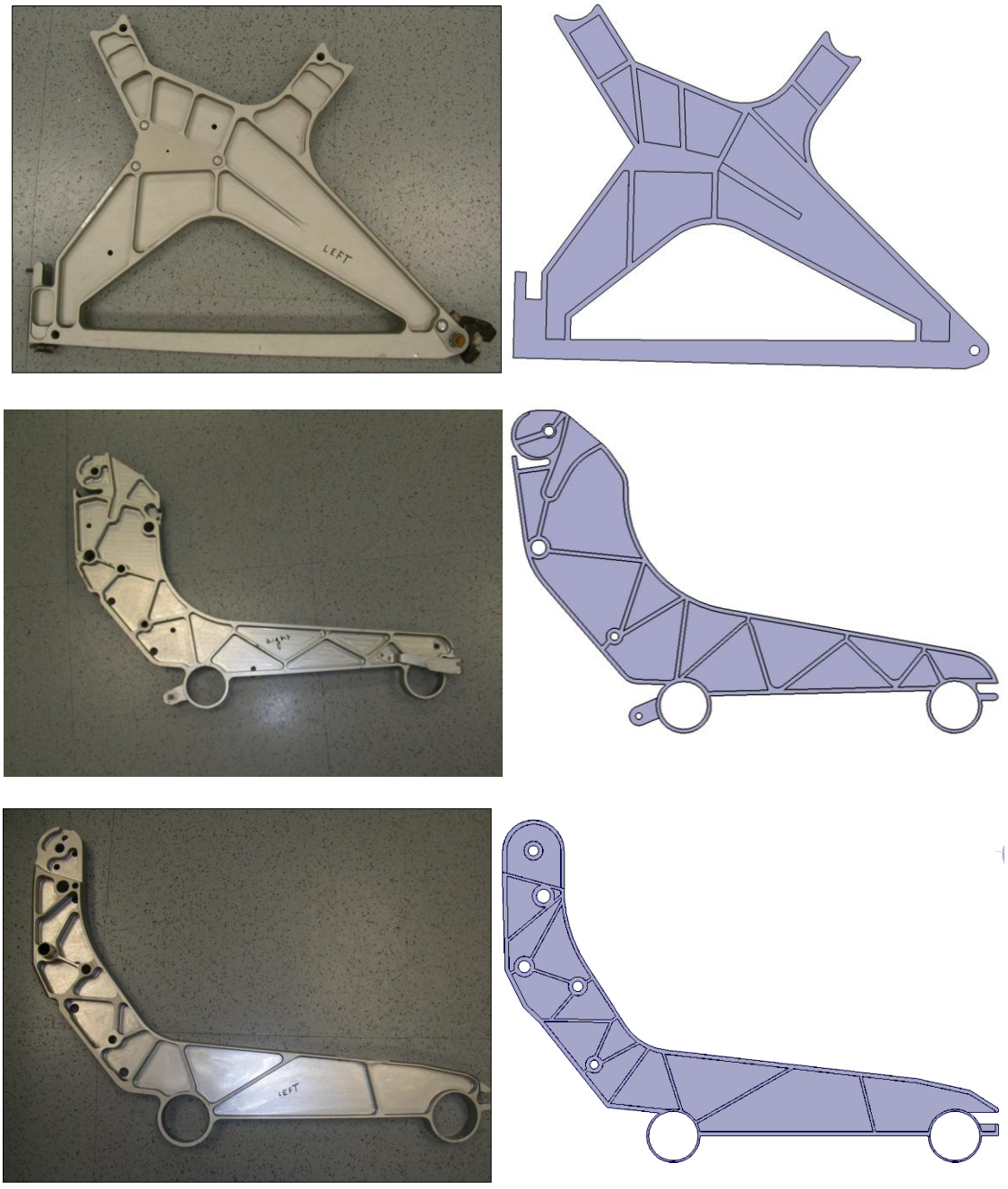

Figure 3-1 Actual component and their cad model

All the individual components were then assembled in CATIA itself to create whole seat assembly. Figure 3-2 and Figure 3-3 shows assembly of seat cad model and comparison of actual seat and cad model.

Figure 3-2 CATIA model of the seat assembly

Figure 3-3 Comparison of Actual seat and cad model

3.4.2 Finite Element Modeling Process

The finite element modeling procedure starting from generation of cad model to final mass check is as follows.

- Obtain CAD data (CATIA, Por-E) for each part or model
- Clean up geometry and prepare for meshing
- Determine connection between adjacent parts and do meshing in accordance with that
- Create FE mesh and check model for quality criteria
- Assign respective material and properties
- Assemble FE mesh parts to create complete Finite element model
- Connect all parts with respective type of connectors
- Check model for free nodes, free edges, mesh overlap or duplicate elements etc.
- Renumber the model as per the convenience
- Check weight of the model and compare with actual seat

3.5 Meshing Procedures

This section describes guidelines those were followed for meshing. These are some of the do's and don'ts those should be followed while meshing so as to avoid some common mistakes.

3.5.1 Meshing of Fillets

Fillets with radius less than 10mm were removed and meshed with sharp edges and an example for this kind of meshing is shown in Figure 3-4.

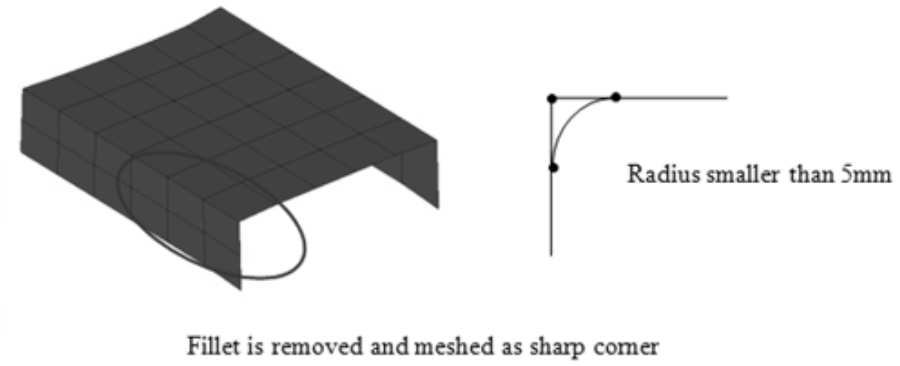

Figure 3-4 Fillet mesh

Fillets with radius larger than 10mm were meshed with at least 2 elements and 1 node on the corner and an example for this kind of meshing is shown in Figure 3-5.

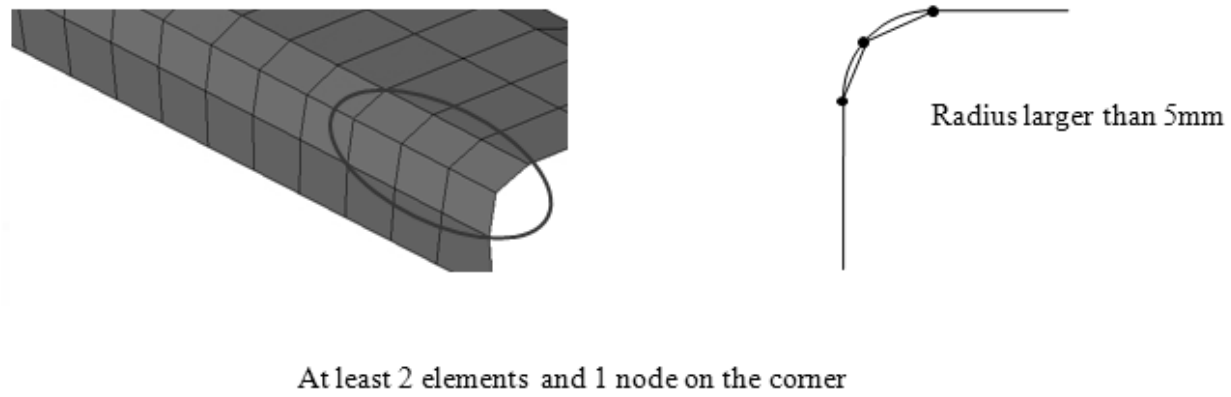

Figure 3-5 Fillet mesh

3.5.2 Meshing of Flange or Rib

Minimum of 3 elements were kept on the sides of flanges or ribs so as to maintain correct stiffness of the part. If only 2 elements used on flanges or ribs then it might be possible that these elements buckle at a lower load just because of incorrect stiffness. This kind of mesh might also succumb to hourglass modes. For an example for this kind of meshing is shown in Figure 3-6.

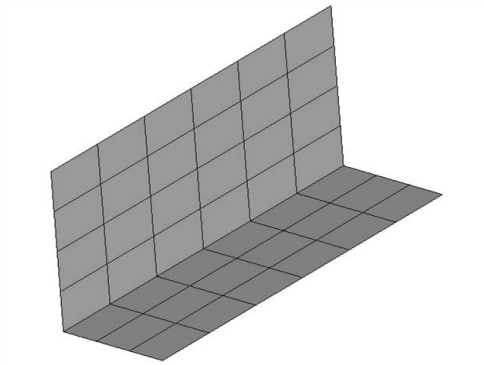

Figure 3-6 Flange or rib mesh

3.5.3 Mesh Transition

Triangular elements were used for the mesh transition. Triangular elements show stiff behavior than quad elements so total number of triangular elements in the model were kept less than 5%. Example of mesh transition is shown in Figure 3-7.

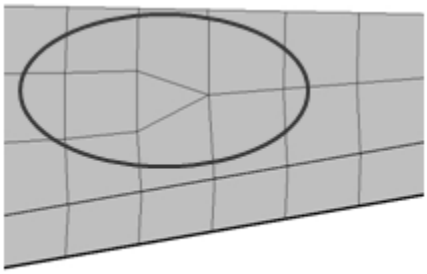

Figure 3-7 Mesh transition

During mesh transition care was taken that triangular elements should not direct towards each other as shown in Figure 3-8. This kind of mesh transition can be avoided by merging these triangular elements.

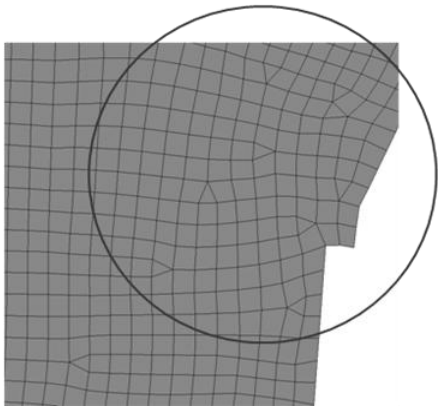

Figure 3-8 Not desirable mesh transition

Try to avoid mesh concentration of triangular elements as shown in Figure 3-9.

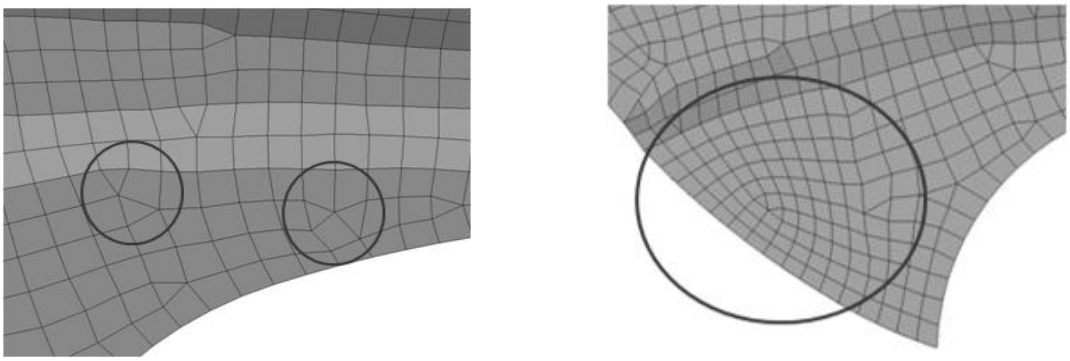

Figure 3-9 Not desirable mesh transition

3.5.4 Mesh Around Hole

Holes with diameter less than 10 mm were removed from the geometry but care was taken to place a node at the center of the hole so as to get exact node for connection. Holes with diameter greater than 10 mm were kept and meshed using washer definition in Hypermesh. While meshing around hole minimum of 6 or even number of nodes were kept. Also care was taken that there are no triangular elements around hole. Desirable and not desirable mesh around hole can be seen in the Figure 3-10.

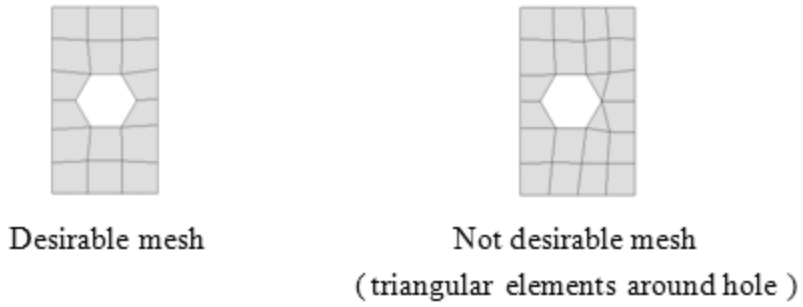

Figure 3-10 Mesh around hole

3.5.5 Element Quality Criteria

This section describes the quality criteria parameters for meshing with their minimum and maximum limits. All these quality criteria's were satisfied before finalizing the mesh.

3.5.5.1 Warpage

Warpage is defined as the angle by which an element or element face (in case of solid elements) deviates from being planar. 15 degrees of warpage angle was used as limit for meshing. Geometrical representation of warpage angle is shown in Figure 3-11.

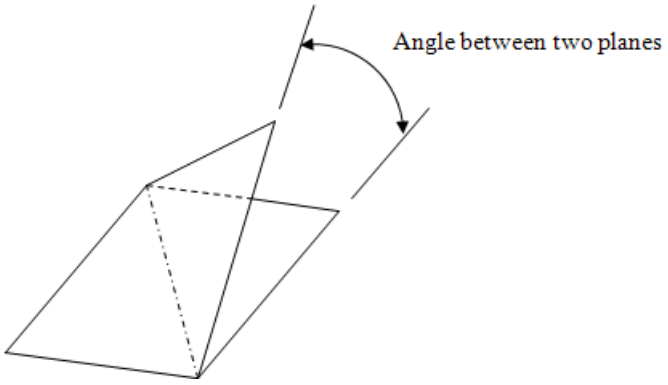

Figure 3-11 Warpage angle [13]

Warpage angle for quad elements is calculated by splitting the quad element twice into two triangular elements using both diagonals and finding the angle between the two planes which the trias form. Maximum of this angle is called as the warpage angle of the element.

3.5.5.2 Aspect Ratio

Aspect ratio is the ratio of breadth and height of an element and calculation for aspect ratio is shown in Figure 3-12. To avoid the instability caused by unusual travel of stress wave, aspect ratio should be less than 5:1.

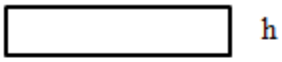

b

Aspect Ratio = b/h < 5

Figure 3-12 Aspect ratio [13]

3.5.5.3 Jacobian

Jacobian ratio is a measure of the deviation of a given element from an ideally shaped element. The jacobian value ranges from -1.0 to 1.0, where 1.0 represents a perfectly shaped element. The ideal shape for an element depends on the element type. The check is performed by mapping an ideal element in parametric coordinates onto the actual element defined in global coordinates. For example, the coordinates of the corners of an ideal quad element in parametric coordinates are (-1,-1), (1,-1), (1,1), and (-1,1). The determinant of the jacobian relates the local stretching of the parametric space required to fit it onto global coordinate space.

3.5.5.4 Skew

Skew angle for quad elements is ninety degrees minus minimum angle made by two lines joining mid points of opposite sides. Skew in quad and trias is shown in Figure 3-13. Skew angle was maintained less than 60^0.

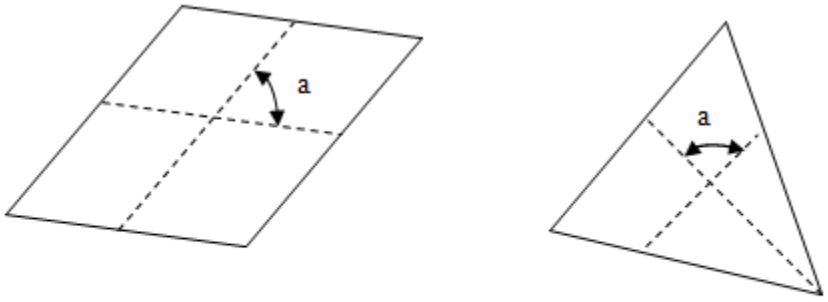

Figure 3-13 Skew angle [13]

3.5.5.5 Length

Minimum side length for elements was maintained above 5mm. This minimum length condition needs to be satisfied so as to keep the computational time step for LS-DYNA above 1 micro second. Following are the calculations [11] for time step with element made with aluminum material and minimum side length of 5 mm.

As an example for aluminum material for simulation of some part following properties can be used

Density $\rho = 2.89xE^{-10}$ ton/mm^3

Young's modulus E = 69000 MPa

Element length $\ell = 5$ mm

Computational time step = Δt

For numerically stable equation

$C = Cn$

where,

C = wave speed through material = $(E/\rho)^{1/2} = (69000/2.89xE^{-10})^{1/2} = 4886249$ mm/s

Cn = numerical stress wave speed = $\ell/\Delta t = 5/\Delta t$ mm/s

Therefore,

$4886249 = 5/\Delta t$

$\Delta t = 1.023xE^{-6}$

$= 1\ \mu$ sec

This quality check is very important to maintain the computational time step of 1 micro second and keep the computational time required in control.

All the quality criteria's with their minimum and maximum allowable values are summarized in Table 3-1.

Table 3-1 Mesh Quality Criteria

Quality Parameter	Allowable Min./Max.
Min. Side Length	5 mm
Max. Side Length	30 mm
Max. Aspect Ratio	5
Min. Quad Angle	45 deg
Max. Quad Angle	140 deg
Min. Tri Angle	30 deg
Max. Tri Angle	120 deg
Max. Warp Angle	15 deg
Min. Jacobian	0.7

3.5.6 Modeling Details of Primary Load Path Components

During development of the FE model particular attention was paid to meshing of primary load path components. Parts like seat pans, tracking tubes, spreaders and legs were fine meshed (5 to 7 mm) to get accurate deformations and load transfer. Element formulation used for shells was Belytschko – Tsay, since it is one of the robust and computationally efficient formulations [14]. Figure 3-14 shows the FE model of primary load path components.

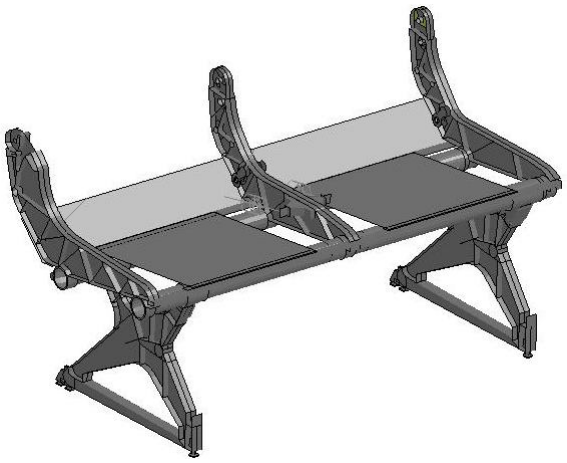

Figure 3-14 Primary load path components

Seat foams undergo very large deformations during high speed impacts and as foam materials are one of the most costly elements for computation, foams were meshed with 10mm to reduce computational time. Rest of the parts which were not critical to performance of the seating system were coarse meshed (10 to 15 mm). Figure 3-15 shows the mesh of seat foam.

Figure 3-15 Seat foam mesh

Certain parts like seat legs or spreaders were machined parts and were having chamfers, fillets and ribs with different thickness to add stiffness to the structure. To capture these features, leg or spreader were divided into different components with different thicknesses. This technique not only helps to maintain stiffness and mass of the structure same as that of test article but also helps to capture the exact nature of geometry. A particular combination of shell and solid elements was intentionally avoided since nodes associated with those two types of elements have different degrees of freedom [14]. When shell and solid elements are connected, rotational degrees of freedom at the adjoining nodes remains free and moments would not get transmit. Modeling details for leg and spreader can be seen in Figure 3-16 and Figure 3-17 respectively.

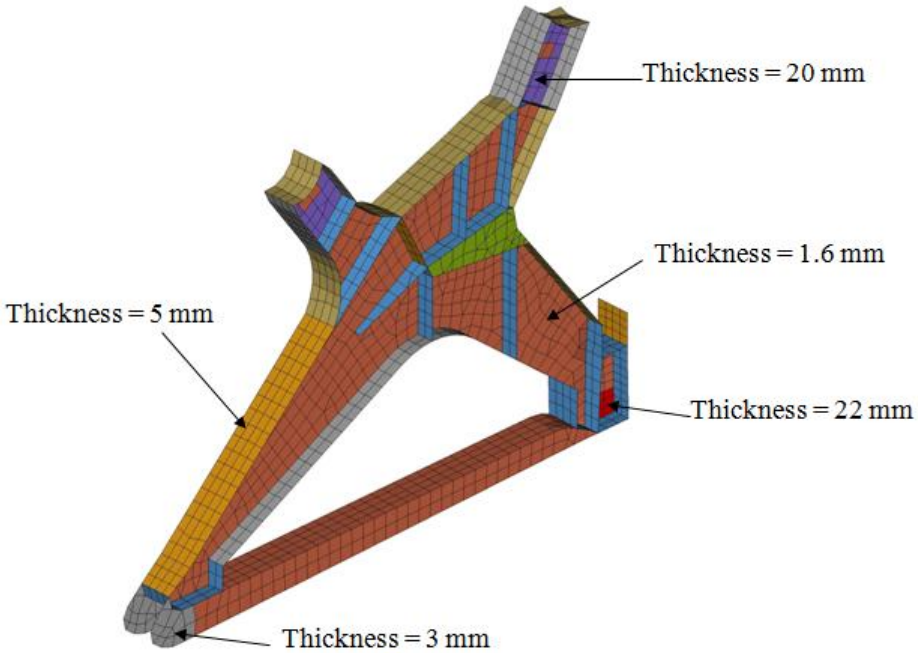

Figure 3-16 Seat leg mesh

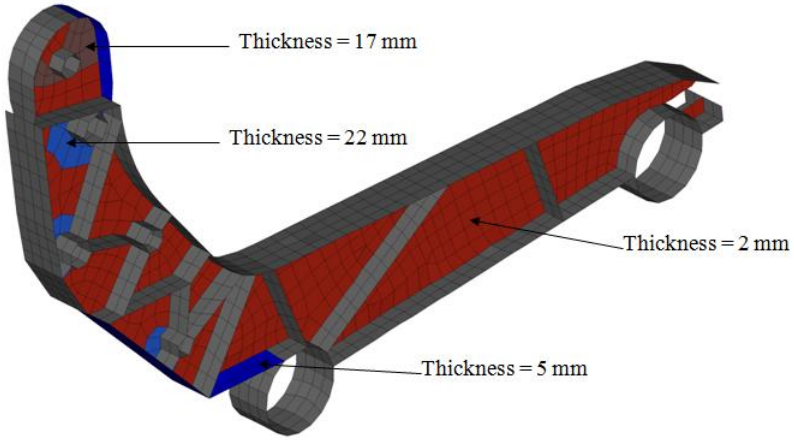

Figure 3-17 Spreader mesh

3.5.7 FE Seat Model

Assembly and connections of the seat FE model was done using the preprocessor Hypermesh 9.0. Figure 3-18 shows the final meshed seat model.

Figure 3-18 Complete seat mesh

3.6 Material Model

LS-DYNA offers various material formulations to model aluminum or steel which are generally used for aircraft seat structures. Material models for elastic materials are considered as the simplest ones. To define this model only Young's modulus and Poisson's ratio are required. This model creates a linear relationship between the stress and strain. During the dynamic event of crash testing some of the materials undergo plastic deformation and these kind of materials can be modeled using an elasto-plastic material model. For these kind of materials stress strain relationship can be used as input to material model and also material failure can be defined based

on the failure strain. Some of the material models used were described with their applications in the following section.

3.6.1 Mat_1 – MAT_ELASTIC

MAT_ELASTIC is an isotropic elastic material and can be used for beam, shell and solid elements. MAT_ELASTIC comes under Hypoelastic material models in Ls-Dyna. For a hypoelastic material relationship between stress and strain is linear. Characteristics of the hypoelastic materials are listed below:

i. Stress strain relationship is linear

ii. Identical to linear elasticity for small strains and small deformations

iii. Path independent (For every different valued of stress, relationship between stress and strain does not change and hence path independent)

Figure 3-19 shows stress – strain relationship for hypoelastic material.

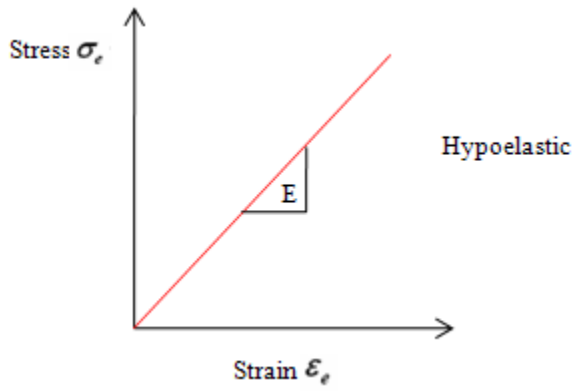

Figure 3-19 Stress – Strain relationship for hypoelastic material [13]

Properties required to define this material in Ls-Dyna are as follows

i. Density

ii. Young's modulus

iii. Poisson's ratio

This material was used for components those can be assumed to remain in linearly elastic region during the course of dynamic event, for example load cells

3.6.2 Mat_20 – MAT_RIGID

As the name of the material suggest, it is a rigid material and used to convert the parts into rigid body. This material also gives option to define local and global constraints on the mass center. Elements which belong to rigid part are bypassed in the element processing and no storage is allocated for storing history variables; consequently, this material type is very cost efficient. [14]

Properties required to define this material in Ls-Dyna:

i. Density

ii. Young's modulus

iii. Poisson's ratio

This material was used for the components which were assumed not to take part in computation of dynamic event and does not deform, for example test sled platform.

3.6.3 Mat_24 – MAT_PIECEWISE_LINEAR_PLASTICITY

This is an elasto-plastic material with an option to define an arbitrary stress versus strain curve and arbitrary strain rate dependency. A material is considered elasto-plastic (or elastic-perfectly plastic) when the inelastic region of the stress-strain diagram is idealized as a straight line [12]. If the material behaves linearly in the elastic range, then the stress-strain diagram consists of two straight lines in the elastic and inelastic regions with different slopes. The hardening is approximated using by piecewise linear. And this is usually defined via discrete points as shown in Figure 3-20.

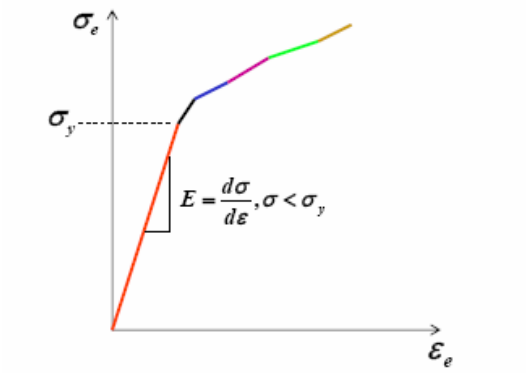

Figure 3-20 Piecewise linear plasticity [13]

Characteristics of this material are described as follows:

i. Perfect plasticity

ii. Bilinear elastic plastic: Stress strain curve is approximated using two straight lines. Only young's modulus and tangent modulus is required to create these lines. An example of bilinear curve is shown in Figure 3-21.

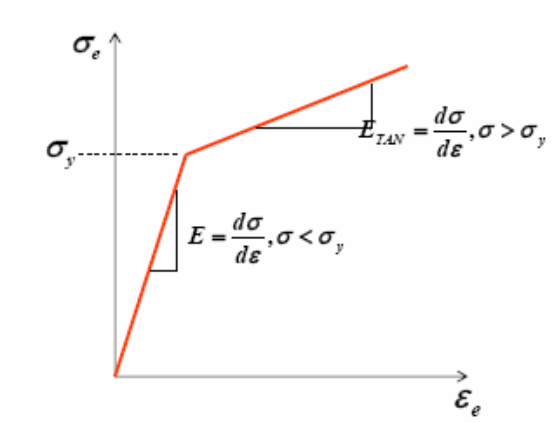

Figure 3-21 Bilinear elastic plastic [13]

iii. Hardening using effective stress/strain points

iv. Hardening using effective stress/strain curve

v. Strain rate effects using a) Cowper-Symonds b) Dynamic scaling of yield stress c) Convenient table input

Properties required to define this material in Ls-Dyna:

i. Density

ii. Young's modulus

iii. Poisson's ratio

iv. Yield Stress

v. Tangent modulus

vi. Load curve defining effective stress versus effective plastic strain

This material was used for most of the structural parts which might show elastic or plastic behavior during the course of dynamic event, for example seat pans, legs, spreaders etc.

3.6.4 Mat_57 – MAT_LOW_DENSITY_FOAM

The material type 57 was used for modeling highly compressible low density foams. Ls-Dyna defines Mat_57 as hyperelastic material model [12]. A hyperelastic material is one for which the stress is obtained from differentiation of a strain energy function wrt the corresponding strain. Stress strain relationship for these kinds of materials is highly nonlinear and is shown in Figure 3-22.

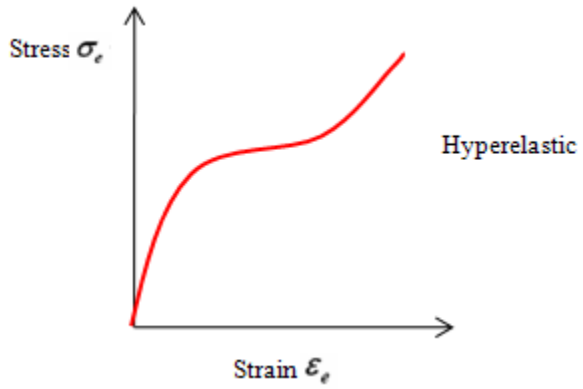

Figure 3-22 Stress – Strain relationship for hyperelastic material [13]

Properties required to define this material in Ls-Dyna:

i. Density

ii. Young's modulus

iii. Poisson's ratio

iv. Load curve defining nominal stress versus strain

3.6.5 Mat_B01 – MAT_SEATBELT

As the name suggests this material was used to model the FE belt segment. Two curves need to be defined for this material representing the loading and unloading characteristics of the seatbelt. And these curves should be force versus engineering strain.

3.6.6 Material Data Source

Material properties for most of the structural parts were taken from Military handbook of materials. Properties for seatbelts and seat foams were from the respective manufacturers.

3.7 Element Types

LS-DYNA offers variety of element formulations for modeling. These elements are categorized as scalar elements, one dimensional, two dimensional, and three dimensional. Some of the properties of these element types are discussed in the following section.

3.7.1 Scalar Elements

Scalar elements are used to represent ballast weights or mass at certain locations. These elements include spring or damper and mass elements. As mass elements represent only lumped mass, there is no stiffness property required.

3.7.2 One-Dimensional Elements

One-dimensional elements include beam and rod elements and have stiffness along a line or curve. Cross section area is required to represent rod elements, and can only carry loads along length i.e. tension and compression.

Beam elements are slightly different than rod elements and have the capability to carry torsion and bending loads in addition to axial loads. Area and moments of inertia are required properties for beam elements. Mass distribution is same for both rod and beam elements and is distributed equally at both nodes.

3.7.3 Two-Dimensional Elements

Two dimensional elements are most widely used because it's easy to mesh them and these elements have variety of robust formulations available. These elements include quadrilateral, triangular and membrane elements. For these elements mass is distributed equally at all the nodes. All the nodes of shell elements have 6 degrees of freedom. Shell thickness and integration points are the only required properties for shell elements. Tri elements shows stiff properties than quad elements and so should be less than 5%.

3.7.4 Three-Dimensional Elements

Tetra, penta and hexa element comes under three-dimensional or solid elements. For these elements mass is distributed equally at all the nodes. These elements can carry tensile, compression and shear loads. These elements use reduced integration scheme to reduce computational time.

3.8 Constraint Modeling

Constraints represent the boundary conditions applied in the model. This includes single and multi-point constraints, contact surfaces, tied connections etc. Following section describes them in detail.

3.8.1 CONSTRAINED_SPOTWELD

These were used to define massless spot welds between the pair of nodes. The spot weld is a rigid beam that connects the nodal points of the nodal pairs. Spot-weld nodes allow nodal rotations. For this FE model spot welds were used to represents the rivets.

3.8.2 CONSTRAINED_NODAL RIGID_BODY

This represents rigid body consisting of the defined nodes. The first node in the nodal rigid body definition has all degrees of freedom and is treated as the master node and rest of as dependent nodes. This nodal rigid body does not allow relative displacement of nodes. These were used in fastener modeling described in section 3.9.

3.8.3 CONSTRAINED_JOINT

Different types of joints such as revolute, translational, spherical etc. are available in Ls-Dyna. Joint stiffness function can also be added to this joint. Following figure shows revolute joint created in FE model.

3.9 Fastener Modeling

A good way to represent fastener in FE is to use a combination of nodal rigid bodies and beams instead of meshing actual fasteners. Beams are particularly used because it is possible to define all the characteristics of fasteners in section card of beams. An example of fastener modeling with beam and nodal rigid bodies is shown in Figure 3-23.

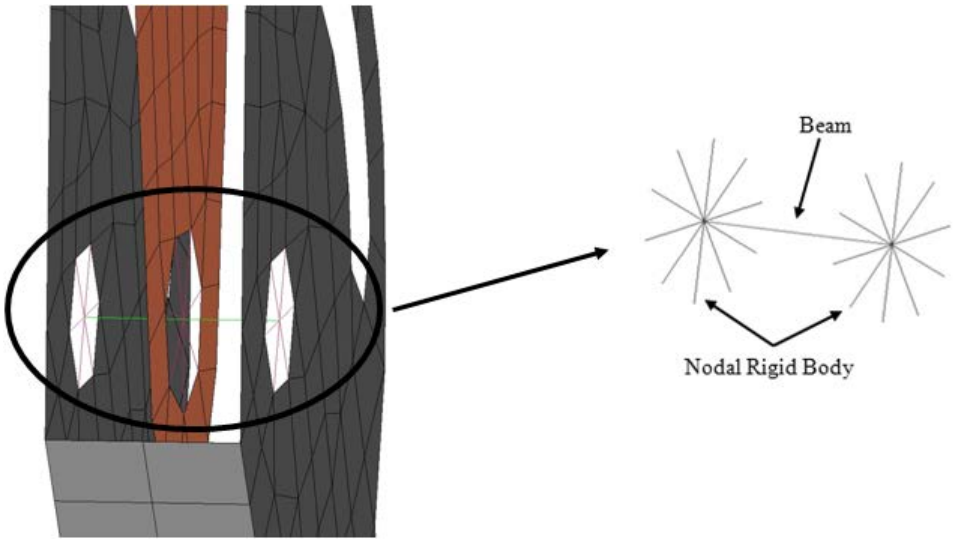

Figure 3-23 Fastener modeling

Element formulation used for beam elements was type2 i.e. RESULTANT_BEAM. Reason behind using element formulation type2 was that this formulation allows defining all characteristics of the fasteners like cross section area, shearing area, moment of inertia in local axis and second polar moment of. These parameters are very important to replicate the exact behavior of beam as a fastener. Figure 3-24 shows the section card for beam elements.

Modify SECTION section 500174 (model 1)

Label 500174 Title: <No section name given>

Type: BEAM

Row\Col	1	2	3	4	5	6	7	8
1	SECID	ELFORM	SHRF	QR/IRID	CST	SCOOR	NSM	
	500174	2	0.0	2.0	0.0	0.0	0.0	
2	A	ISS	ITT	IRR	SA			
	49.48	194.8	194.8	389.0	44.5			

Figure 3-24 Section card for beam elements

Figure 3-25 shows the cross section for circular beam and its calculations [14].

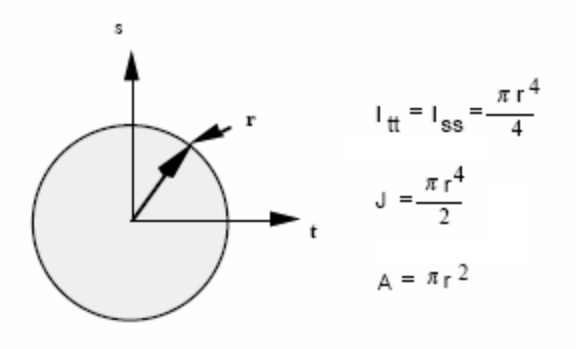

Figure 3-25 Properties for circular cross section beam [14]

3.10 Cushion Modeling

A material type 57 i.e. MAT_LOW_DENSITY_FOAM was used for modeling highly compressible low density foams. Ls-Dyna defines MAT_57 as hyperelastic material model. Constant stress element formulation was used for solid elements to reduce the computational time. Figure 3-26 shows the FE seat cushion model.

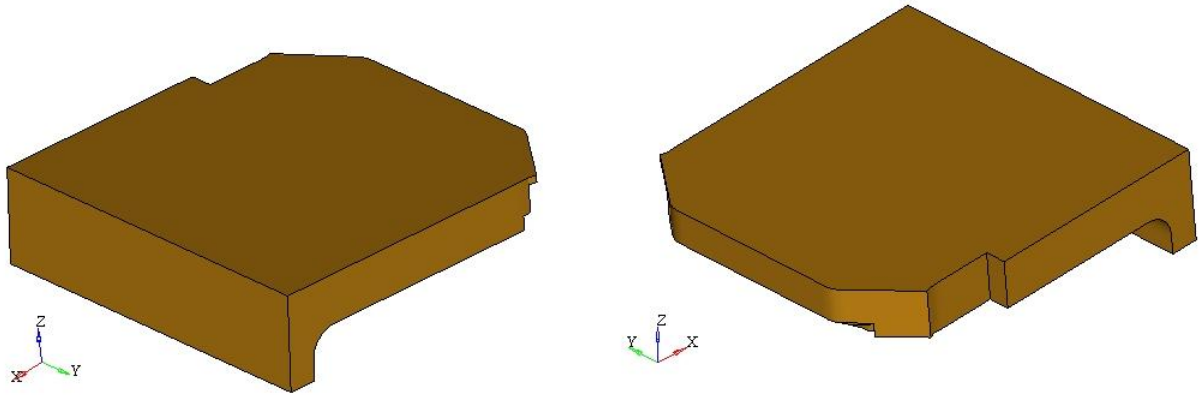

Figure 3-26 Seat cushion

This MAT_57 needs an input of stress - strain curve from actual foam material to replication the compressive nature of seat foam. To generate this material data component test was conducted on seat foam material. These component tests were conducted in Wichita State Composites Laboratory and general setup for test is shown in Figure 3-27 (Note - Figure 3-27 shows only general setup and foam component in the picture is not the actual foam).

Figure 3-27 Seat foam test setup

A high loading rate of 30 in/sec was used for the dynamic testing of foam material and properties generated form testing were used to model FE seat cushion and shown in Figure 3-28.

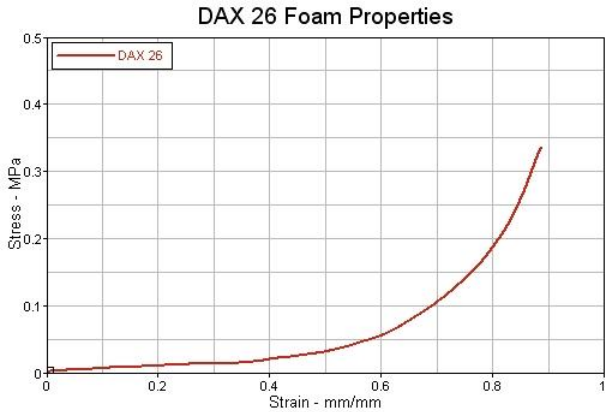

Figure 3-28 Seat foam stress - strain curve

3.11 Seatbelt Modeling

FE seatbelt was modeled by the combination of FE part and 1D seatbelt segments. 1D seatbelt segments were used to model seatbelt webbing. Material card used for 1D segments was MAT_B01 i.e. MAT_SEATBLET. Force versus engineering strain curves obtained through testing of seatbelt webbings were used as input to material model. Figure 3-29 shows the FE seatbelt model.

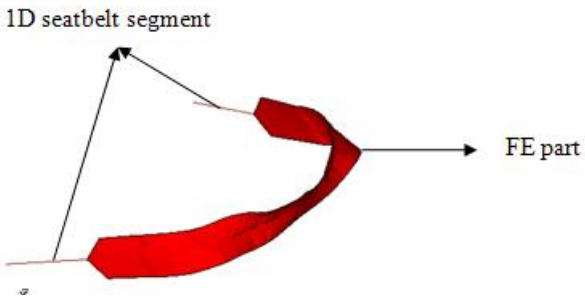

Figure 3-29 FE seatbelt model

Loading and unloading characteristics of belt were represented in following Figure 3-30.

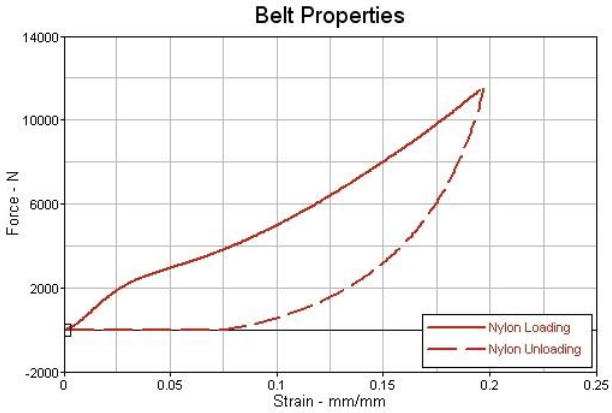

Figure 3-30 Seatbelt properties

3.12 Contact Modeling

Contact modeling is one of the important parts in FE modeling of dynamic event of crash testing. Results of the finite element simulations are highly dependent on correct modeling of contact between different components of FE model. LS-DYNA provides different ways of contact modeling using *CONTACT card. Interactions between the seat and the occupant, between seat components, occupant self contact, occupant-to-occupant contact, and interactions with other objects in the aircraft interior can be modeled using contact definitions.

For the events with large deformations like crash simulations, it is difficult to find out the regions of contact until and unless have one simulation. For this kind of simulations LS-DYNA has the option of automatic contact definitions. Automatic contacts can detect penetration from either side of a shell element. This section describes the different types of contact definitions along with control parameters for *CONTACT card

3.12.1 One Way Type Contact

This type of contact checks only selected slave nodes for penetration through master segment and hence called as one-way type contact. This contact definition transfers compression loads between parts in contact and if contact friction is defined, it also transfers tangential loads.

3.12.2 Two Way Type Contact

For two way contact definitions both master and slave nodes are checked for contact penetrations. Treatment used for slave and master segments is symmetric. These types of contacts are more costly than one way type and approximately take twice time as compared to one way type contacts.

3.12.3 Single Surface Contact

Single surface contact defines contact between all the parts in the list and also self contact of each part. These contact types are very easy to define as only slave part list is required and no master surface is required. These work very well and are reliable.

3.12.4 Contact Stiffness Calculation

Force applied by master segment on slave nodes is dependent on the stiffness of the contact. Contact algorithm generates linear springs between master nodes and slave nodes. LS-DYNA has two methods namely penalty based approach and soft constraint based approach for calculation of contact stiffness which are discussed as below.

3.12.4.1 Penalty Based Approach

Penalty based method is the default method in contact card of LS-DYNA. Contact stiffness calculation is dependent on materials of the parts in list and their size. This method is good option when parts in the contact are more or less of the same materials. If very hard and soft like metal and foam are in contact then there might be a chance of contact failure.

3.12.4.2 Soft Constraint Based Approach

Soft constraint based method is dependent on global time step and mass of the nodes those are in the contact segments. As this method is not dependent on material constants it is good option for treatment of contact between dissimilar materials.

3.12.5 Contact Parameters

*CONTROL_CONTACT offers various parameters to control and improve the contact behavior in LS-DYNA. These parameters are described in the following section.

3.12.5.1 Thickness Offset

Whenever sheet metal components are meshed at the mid-surface, this option creates the surface for contact and projects it to its actual place by its thickness value.

3.12.5.2 Contact Sliding Friction

Contact sliding friction is defined by the static and dynamic friction coefficient. For crash simulation these coefficients are set equal to avoid noisy outputs.

3.12.5.3 Penalty Scale Factor

Contact stiffness values can be artificially manipulated by using Penalty scale factors, SFS and SFM.

3.12.5.4 Contact Thickness

This is good option to artificially remove initial penetrations in contact groups. This option gives a way to manipulate the actual thickness of the parts in contact.

3.12.5.5 Viscous Damping

Viscous damping is used to damp out the noisy outputs. Generally very soft materials like foams or honeycombs tend to create instabilities due to noisy contacts. LSTC recommends a

value of VDC between 40 and 60 (corresponding to 40 to 60% of critical damping), to improve the model stability.

3.13 Connections/Implicit Checks

Once the model has been meshed and material properties assigned to each component, next step is to connect all the parts with appropriate connection type. It is very important step to check whether these parts are properly connected or any one is free. Implicit eigenvalue analysis is an important tool to check any missed connections and unconstraint degrees of freedom. Two control cards needs to be defined for implicit analysis and those are described as follows: CONTOL_IMPLICIT_GENERAL – This card was used to activate the implicit analysis and initial time step size for implicit analysis was also defined in this card.

CONTOL_IMPLICIT_EIGENVALUE – This card activates eigenvalue analysis and number of eigenvalues to be extracted can be defined in this card. Figure 3-31 shows one of the modes of the eigenvalue analysis.

Figure 3-31 Eigenvalue analysis for connection checks

3.14 Hourglass

Hourglass or Spurious or Zero energy modes corresponds to any motion that is not a rigid body motion and results in no straining of the element. These modes occur due to reduced integration scheme used for the numerical simulation.

Hourglass mode can occur in single element or mesh of elements. It is called hourglass mode because of its physical shape.

An example of hourglass mode for a four node element:

There are 8 independent deformation modes [16] shown in following Figure 3-32.

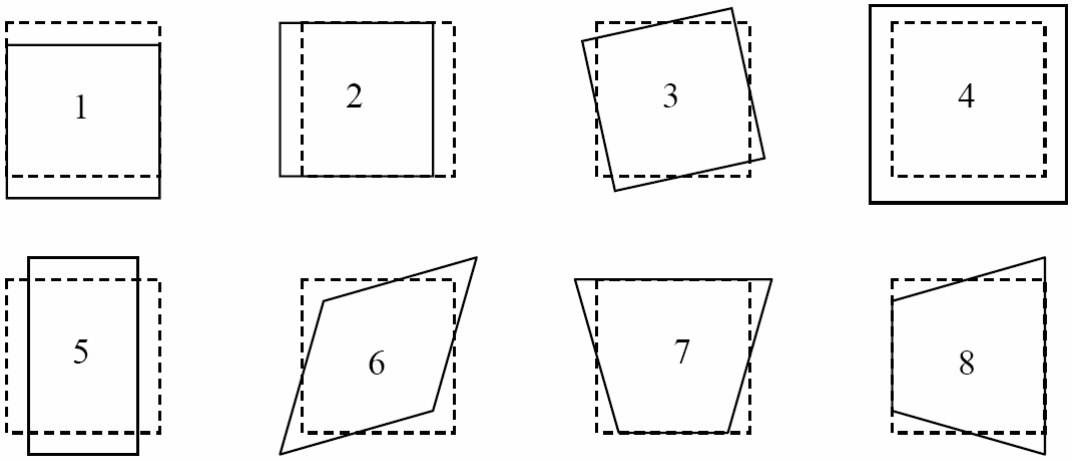

Figure 3-32 Deformation modes [16]

Modes 1 to 3 : rigid body motions, Modes 4 to 6 : non zero energy modes

Mode 7 and 8 : zero energy modes if one point integration is used, because a single Gaussian point at the center does not sense these modes. At the center these two spurious modes will disappear if higher order Gaussian integration (2 or higher) is used.

3.15 Load Application

For this dynamic crash testing load was applied as a deceleration pulse to sled. This method simulates the physical event, as experienced by the occupant. Figure 3-33 shows the deceleration pulse applied to the system.

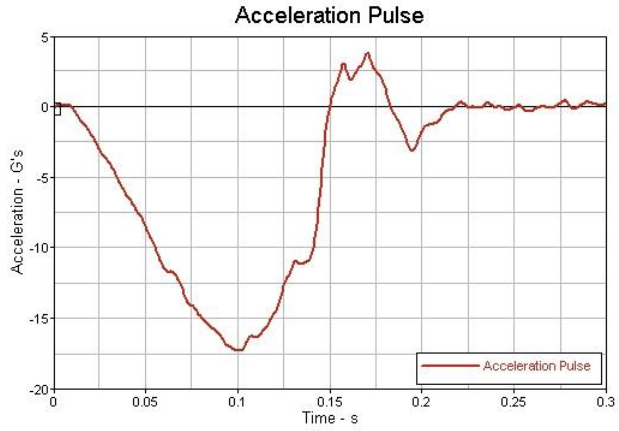

Figure 3-33 Acceleration pulse for test II condition

Gravitational acceleration was applied using the card LOAD_BODY. Acceleration curve used for gravity loading is shown in Figure 3-34.

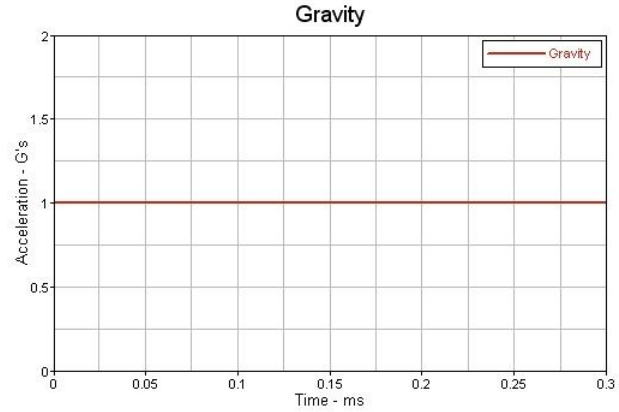

Figure 3-34 Gravitational acceleration

3.16 Occupant Models

FTSS HII 50th% occupant FE model was used for this simulation. FTSS HII 50th % FE model was specifically developed and validated for aerospace applications by FTSS in working with FAA and NIAR at Wichita State University. The FE model of the dummy has the same injury sensors as in the actual dummy: accelerometers in head, chest and pelvis, load cells in lumbar spine and femurs to measure forces and moments and a potentiometer in chest to measure chest deflection. Figure 3-35 shows the actual and FE FTSS HII 50th% occupant model.

Figure 3-35 Actual and FE FTSS HII 50th% occupant model

3.17 General Analysis Control Parameters

These are some of the specialized control parameters that can control, accelerate and terminate an analysis. These also are used to enhance the performance of the software and reduce the computational time.

CONTROL_TERMINATION: This card is used to stop the job in terms of termination time.

CONTROL_TIMESTEP: This card allows setting structural time step size using different control parameters. Mass scaling options are also available in this card. Also a time step scale factor can be defined to determine the minimum time step value.

CONTROL_CONTACT: The purpose of this card is to change the defaults for computation with contact surface. Different control parameters such as initial penetration check, penalty stiffness for contact or contact with soft options can be activated by this card.

CONTROL_HOURGLASS: This card gives different control parameters for hourglass control for both shell and solid element formulations.

3.18 Data Outputs and Their Filters

*DATABASE card was used to generate the output files containing results information. Data was generated in both ASCII and Binary format with a time interval of 1 ms. Table 3-2 shows the database cards used and their output results. Data from both simulations and actual test shows some noise in output channels. SAE J211 filters of respective frequency class were used to filter the data.

Table 3-2 Database Outputs

Database Card	**Output Result**
ELOUT	Element Data
GLSTAT	Global Data
JNTFORC	Joint Force Output
MATSUM	Material Energies
NODOUT	Node Output
SBTOUT	Seat Belt Output
SECFORC	Cross Section Output

CHAPTER 4

SLED TEST AND SIMULATION SETUP

This chapter describes the sled test and simulation setups. Tests were conducted at the sled facility of Civil Aero Medical Institute (CAMI). Table 4-1 shows the test matrix.

Table 4-1 Test Matrix

Test No	Belt Type	Floor Angle (Deg)	Peak Acceleration (g's)	Crash Pulse
07005	2 pt	0	16	PART 25-562
07011	2 pt	60	14	PART 25-562

4.1 Test No. 07005

This test was conducted at the sled facility of Civil Aero Medical Institute (CAMI). A forward facing seat was used with one FTSS H II 50th % dummy sitting on right side of the seat. Table 4-2 shows the test summary.

Table 4-2 Summary Test No. 07005

Test No	07005
Pulse	PART 25-562 Horizontal
Floor Angle	0 deg
Floor Deformation	No
Yaw Angle	No
Test Dummy	H II 50th %
Simulation Dummy	FTSS H II 50th %
Type of Belt	2 pt

Figure 4-1 shows the comparison of test and simulation setup.

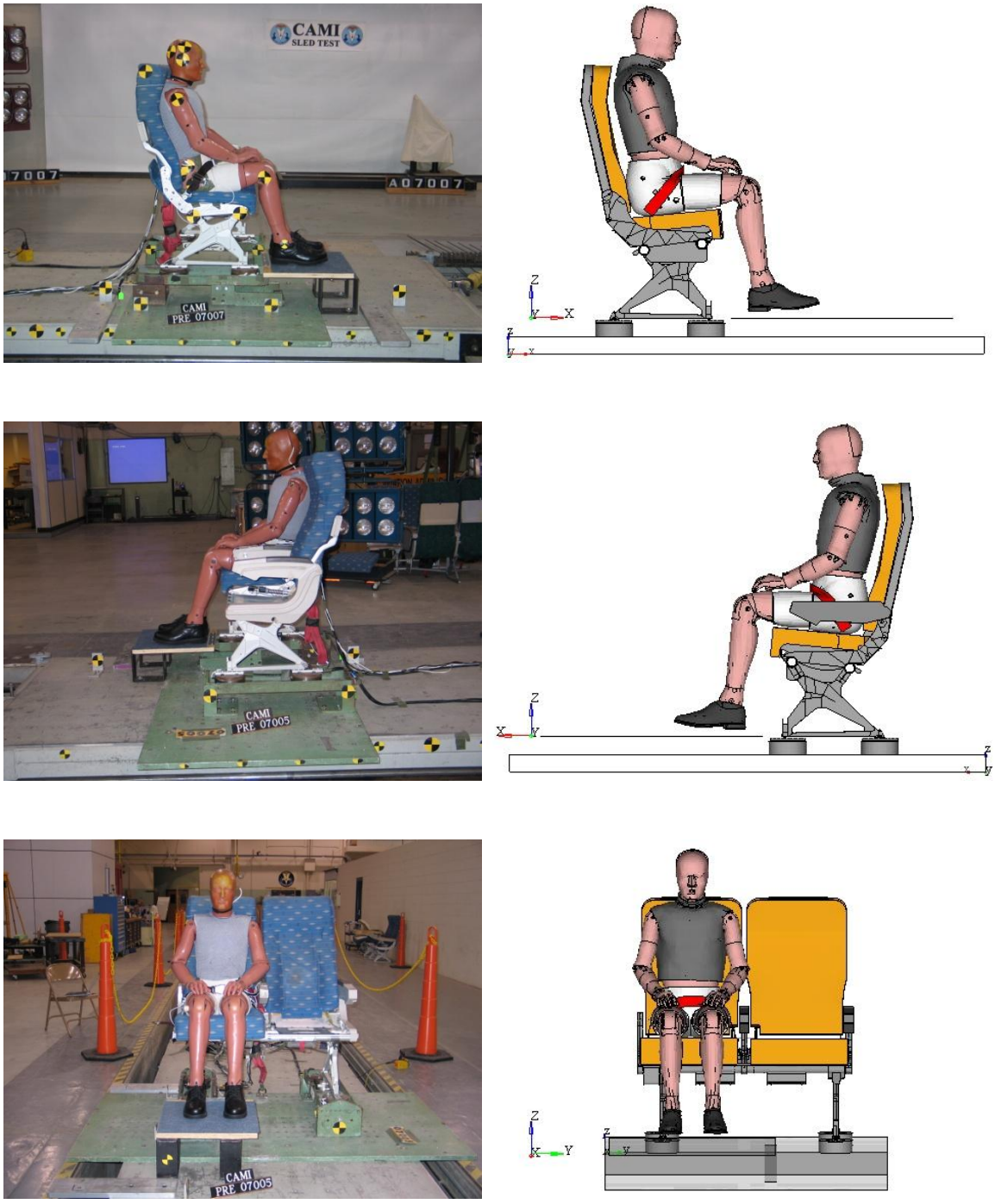

Figure 4-1 Test and simulation setup comparison

Acceleration Pulse used for this test was as per 14 CFR PART 25-562 and generated from actual 0 deg forward sled test. Figure 4-2 shows the acceleration pulse.

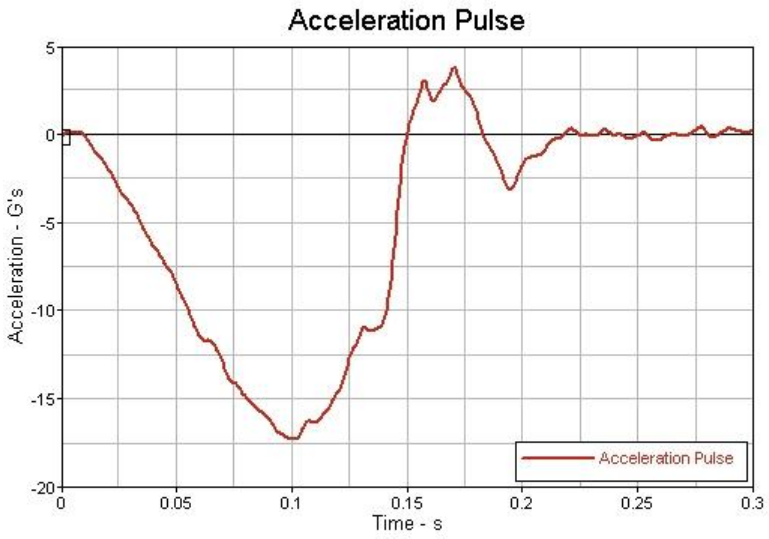

Figure 4-2 Test 07005 acceleration pulse

4.2 Test No. 07011

This test was conducted as per PART 25-562 Test I condition and summarized in the Table 4-3.

Table 4-3 Summary Test No. 07011

Test No	07011
Pulse	PART 25-562, Vertical
Floor Angle	60 deg
Floor Deformation	No
Yaw	No
Test Dummy	H II 50th %
Simulation Dummy	FTSS H II 50th %
Type of Belt	2 pt

Comparison of simulation and Test setup is shown in Figure 4-3.

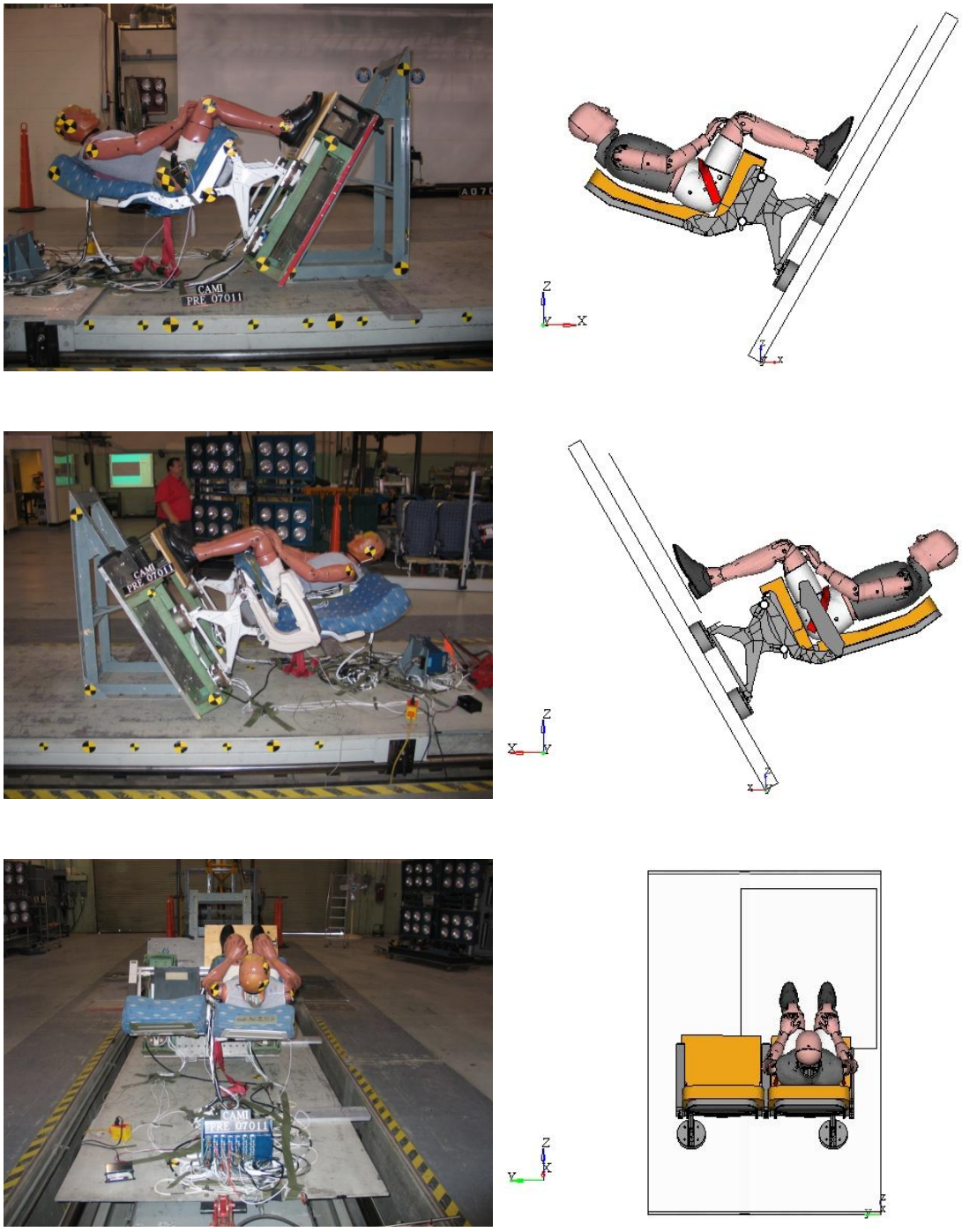

Figure 4-3 Test and simulation setup comparison

Acceleration pulse generated from the actual 60 deg sled test was used for simulation model and is shown in Figure 4-4.

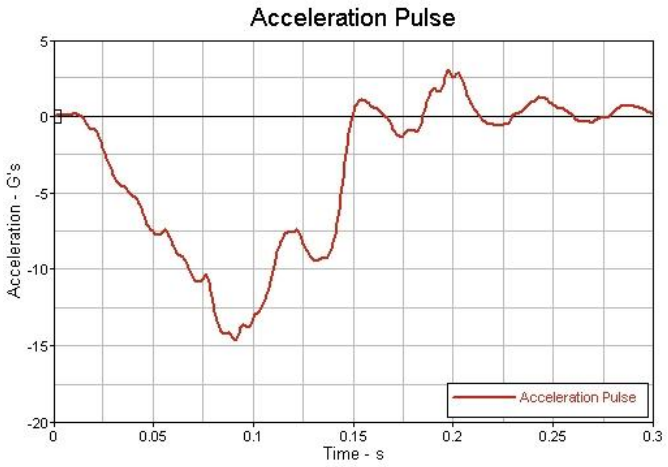

Figure 4-4 Test 07011 acceleration pulse

CHAPTER 5

RESULTS AND VALIDATION

5.1 Validation Criteria

As with any form of analytical modeling, validation of the seat/restraint model is a key step in determining whether the model is acceptable for use in certification. By definition validation is a process of testifying that a process or event is compliant with the standard or rules. Any developed numerical model needs to be validated before it is used for further studies. Validation is done against the actual sled test results.

Validation of simulation model was done in two categories as described in the following section.

5.1.1 Dummy Kinematics

Dummy kinematics from simulation and testing were visually compared. Also frames were captured at certain time intervals compare exact behavior of simulation models with testing.

5.1.2 Validation of the Profiles and Quantitative Comparison

With the increasing role of computational modeling in safety assessment, improved methods are needed for comparing computational results and experimental measurements. In order to quantitatively measure the uncertainty in the experimental data, a number of validation or error metric methods were considered. These methods consist of computable measures that can quantitatively compare experimental and/or computational results over a series of parameters to objectively assess computational accuracy and or experimental uncertainty over the traditional qualitative graphical comparison. The applications of these validation metrics in this study include the evaluation of model quality.

There are many validation metric methods used. Among them Sprague and Geers method was selected based on its intuitive score values, easy implementation, and bias towards experimental data which is consistent with certification procedures.

5.1.2.1 Shape Error

The Sprague and Geers method considers a magnitude error factor that is insensitive to phase discrepancies, a phase error factor that is insensitive to magnitude discrepancies. A shape error is the difference of phase between two profiles and can be seen in Figure 5-1.

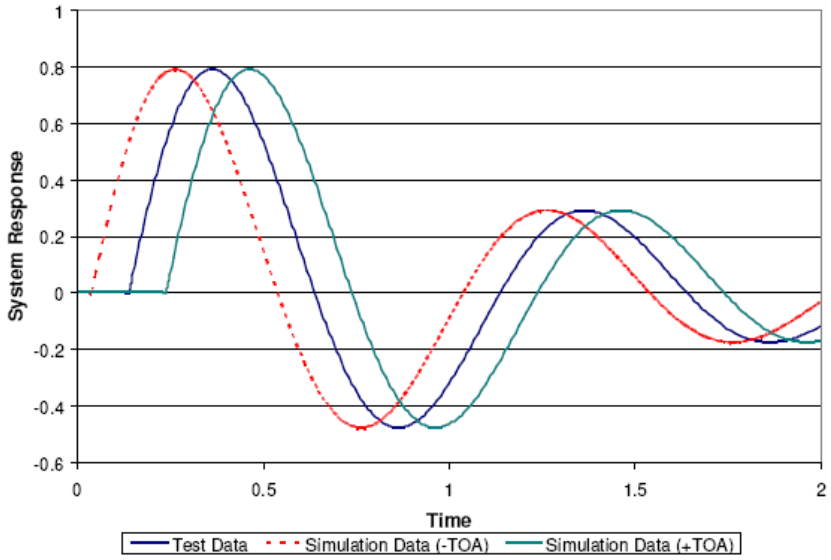

Figure 5-1 Shape error [17]

5.1.2.2 Magnitude Error

The relative error method is a very common or well known metric used to compare two values quantitatively in the form of a percentage difference. This method does not consider time variations or phasing, so it is only good to compare the maximum magnitude of a response as shown in Figure 5-2.

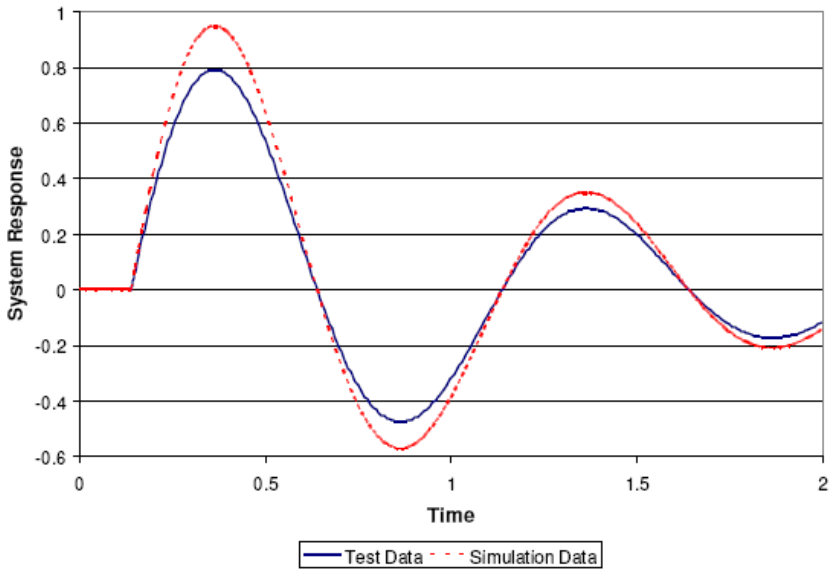

Figure 5-2 Magnitude error [17]

The magnitude error is given by the following expression:

$$\text{Magnitude error} = \frac{g(t) - f(t)}{f(t)}$$

f(t) = benchmark history or reference data

g(t) = candidate solution or data to compare

5.2 Validation of Simulation Model for Test No. 07005

As discussed earlier in this chapter, kinematic comparison and profile validation were used as the validation tools. These two methods were applied to each test and simulation comparison and results are discussed in section 5.2.1 and 5.2.2.

5.2.1 Kinematic Comparison

Comparison of kinematics till 190 ms is shown in Figure 5-3. Kinematic frames shows that the simulation dummy followed the same pattern as that of test dummy. Movement of head and pelvis from simulation model follows closely to that of test. Structural deformation of seat back was also observed same as that of test article.

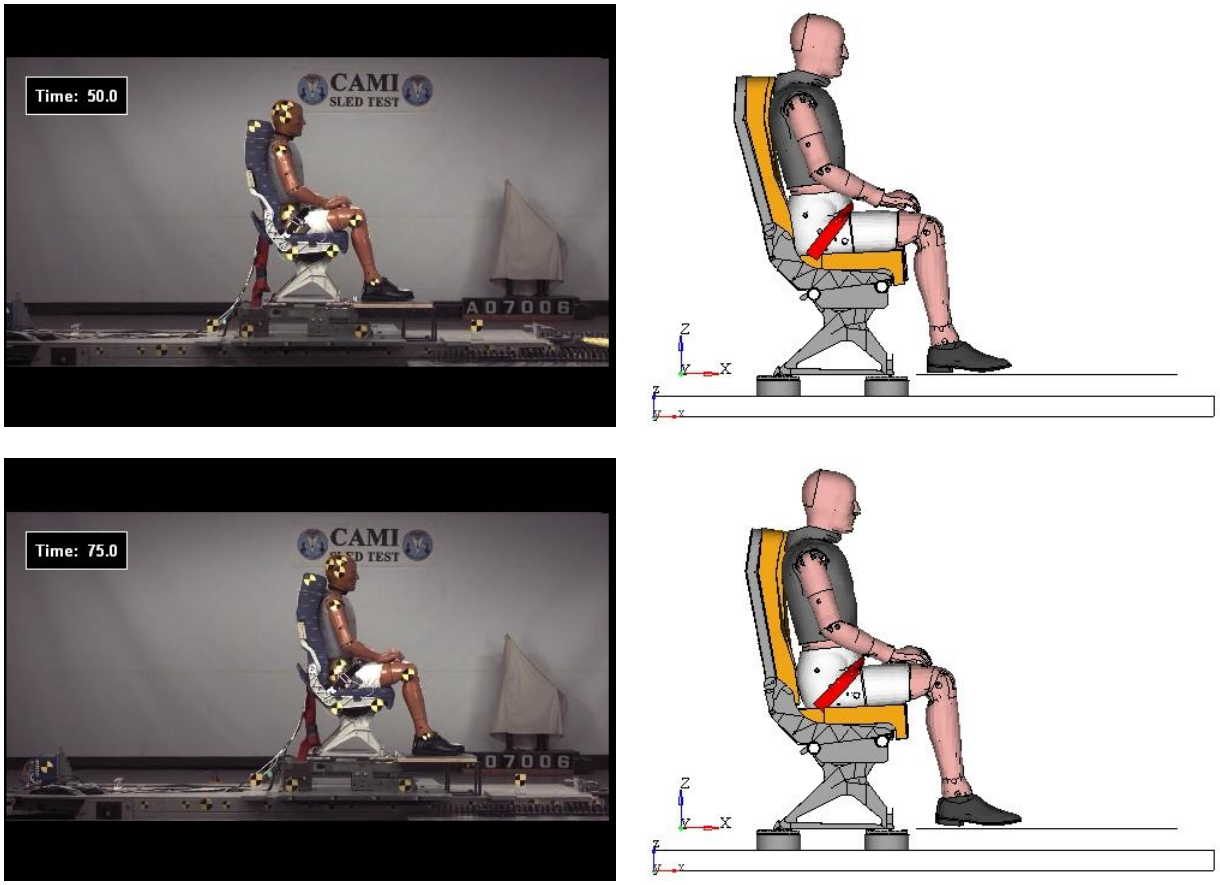

Figure 5-3 Kinematic comparison for test no. 07005

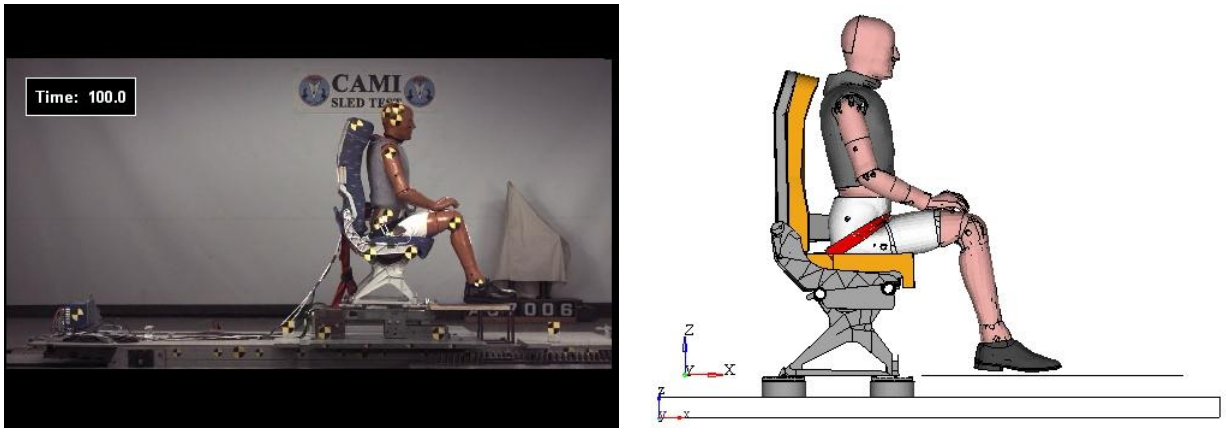

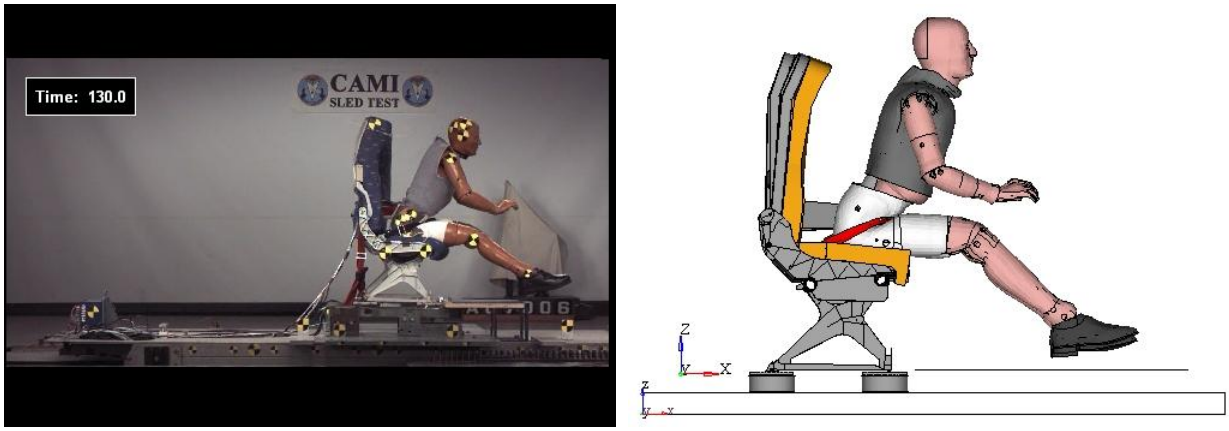

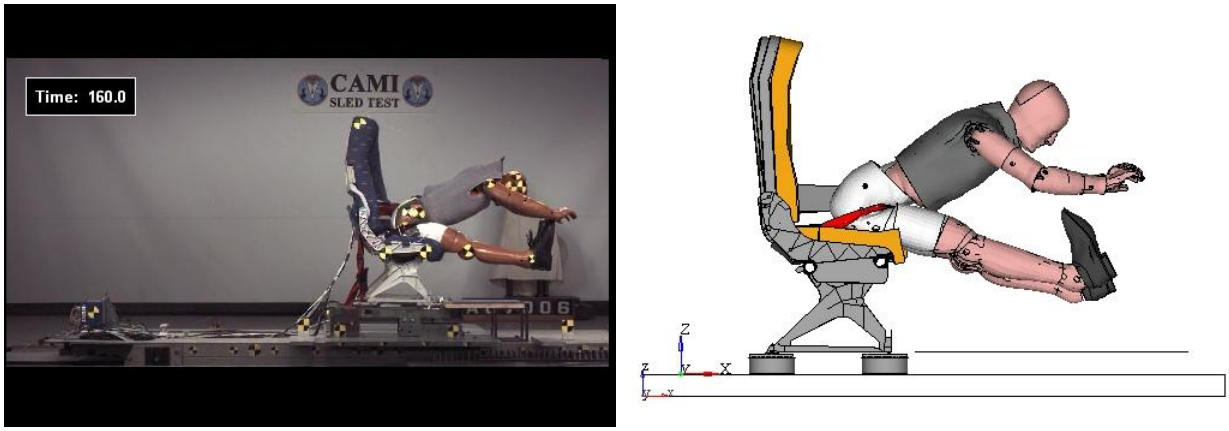

Figure 5-3 Kinematic comparison for test no. 07005 (cont'd)

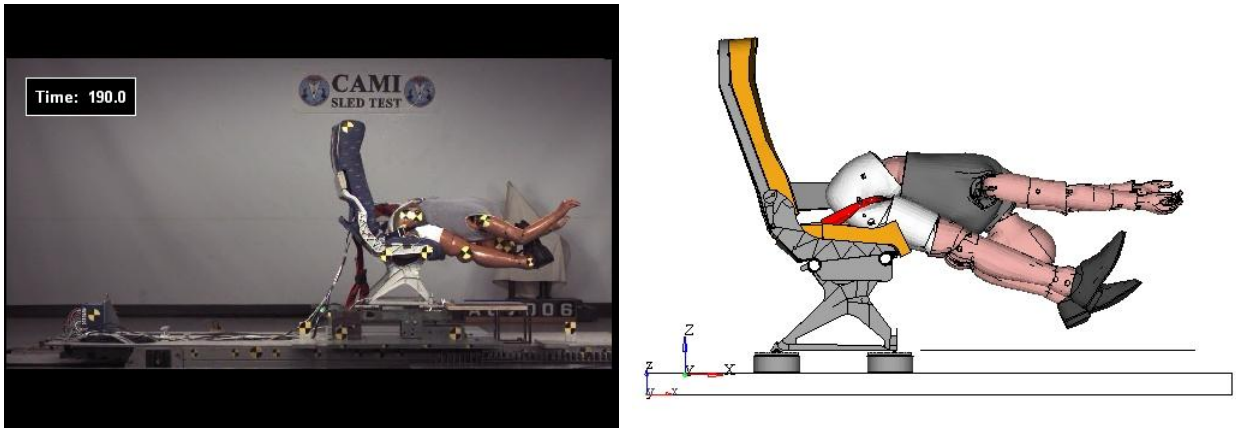

Figure 5-3 Kinematic comparison for test no. 07005 (cont'd)

5.2.2 Validation of the Profiles and Quantitative Comparison

Data channels used for validation of profiles were enlisted as follows:

a) Head acceleration

b) Chest acceleration

c) Pelvis acceleration

d) Lumbar force and moment

e) Belt forces

f) Floor reaction forces

Out of these listed channels, importance of channel changes as per the test condition. For example for Test I condition lumbar Z force is very important as compared to Test II condition. For 0 deg forward test dummy acceleration values, belt forces and floor load reactions are important channels.

For this test dummy was sitting on right side of seat making right side load cells more important that left side as these load cells were heavily loaded. Figure 5-6 shows the comparison for floor reaction peak forces and right side load cells are correlated very well. Table 5-1 shows the profile validation results obtained using Sprague and Geers method. Peak values of each channel are also compared and shown in Figure 5-4, Figure 5-5 and Figure 5-6.

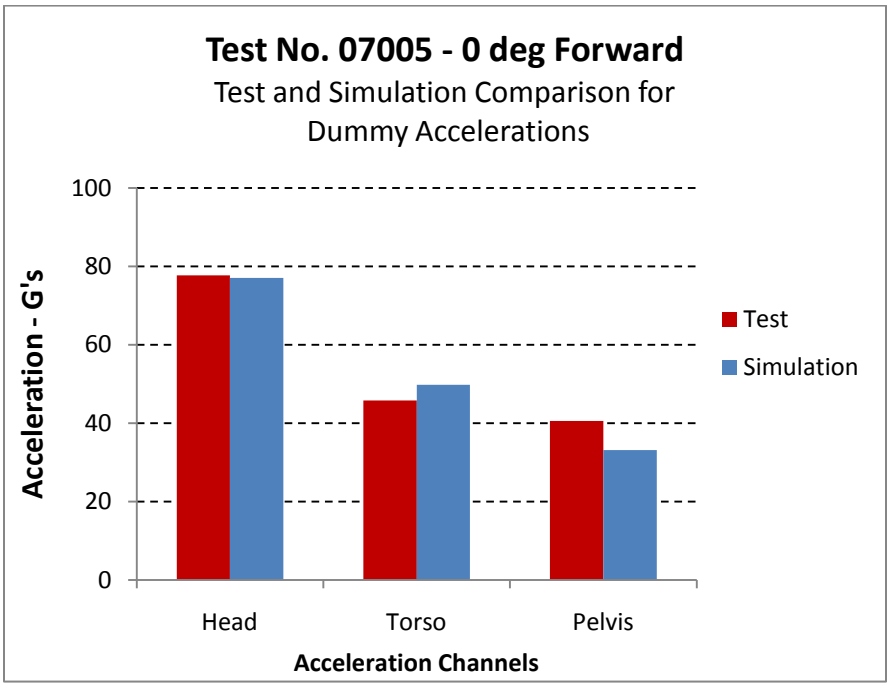

Figure 5-4 Test and simulation comparison for dummy acceleration

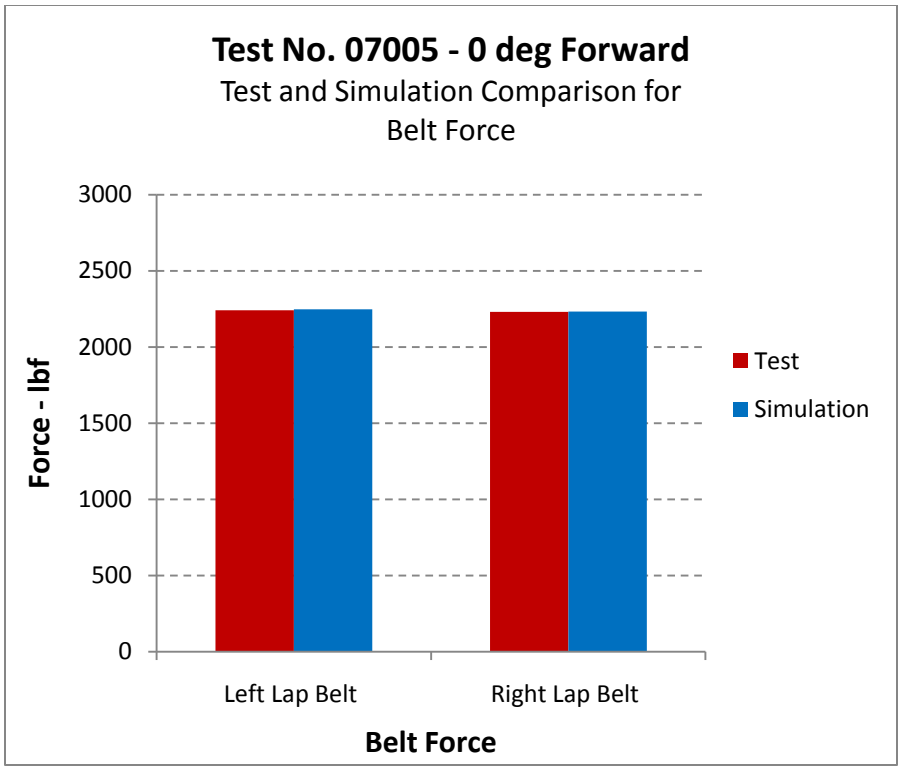

Figure 5-5 Test and simulation comparison for belt force

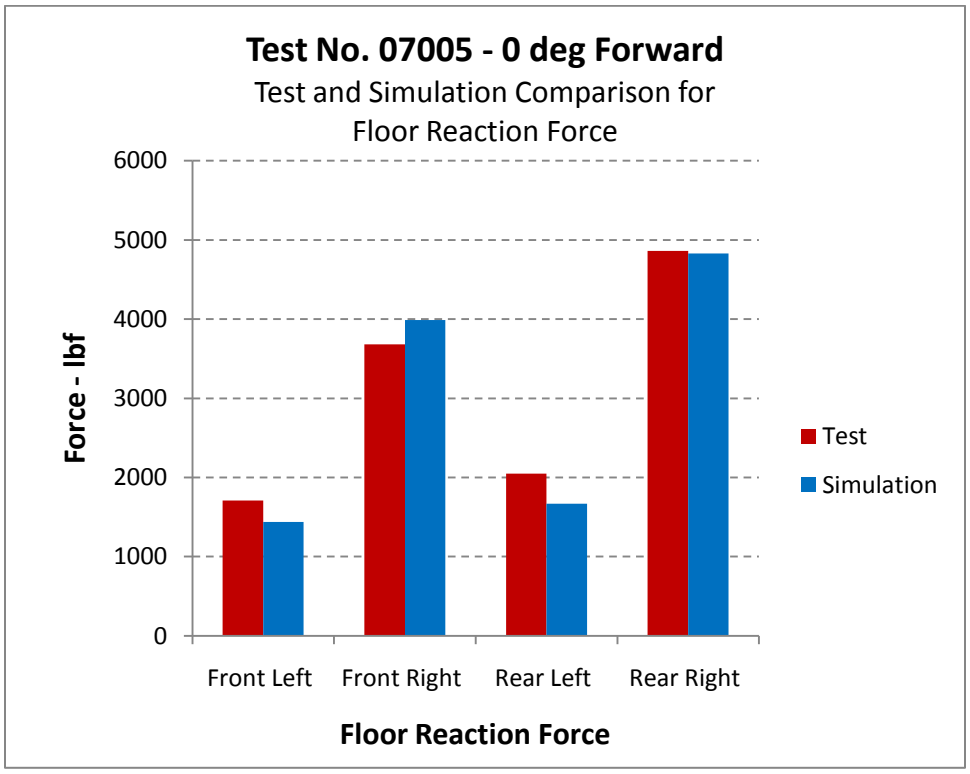

Figure 5-6 Test and simulation comparison for floor reaction force

Table 5-1 shows the profile validation results obtained using Sprague and Geers method. All of the critical simulation output channels (highlighted with bold letters) showed good comparison with that of test data and have the difference of peak values less than 10%. Shape error values were also less indicating that simulation model followed closely the load transfer profile of test.

Table 5-1 Profile Validation Results for Test No. 07005

Component	Output channel	Mag. Error	Shape Error
Head	Head Resultant Acceleration	1%	6%
Torso	Torso Resultant Acceleration	9%	14%
Pelvis	Pelvic Resultant Acceleration	18%	10%
Lumbar	Lumbar Force X	9%	9%
	Lumbar Force Z	1%	21%
	Lumbar Moment Y	5%	21%
Lap Belt	**Left Lap Belt**	**0%**	**8%**
	Right Lap Belt	**0%**	**8%**
Floor Loads	Front Left Leg	15%	19%
	Front Right Leg	**9%**	**9%**
	Rear Left Leg	18%	20%
	Rear Right Leg	**1%**	**9%**

The result comparison for front left and rear left loads shows a higher % differences but this is just because that the original test values for these channels were very small and so even small difference between test and simulation makes the % difference a big value.

Head path is also one of the important parameter of validation for 0 deg forward tests as it defines the total dummy movement envelopment. Comparison of simulation with test shows good correlation with magnitude of less than 5% and can be seen from the Figure 5-7.

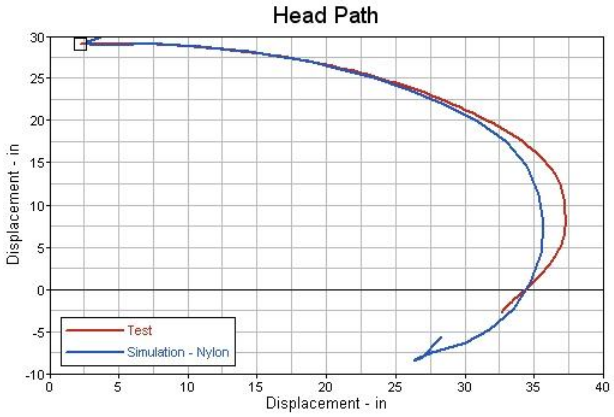

Figure 5-7 Head path comparison for test no 07005

5.3 Validation of Simulation Model for Test No. 07011

Results for test no. 07011 were validated in this section using the same procedures explained in section 5.2 .

5.3.1 Kinematic Comparison

For this test also kinematic frames were taken till 190ms and are shown in Figure 5-8. Overall movement of dummy was observed to be same as that of test. Kinematic frames comparison shows that the simulation dummy followed the same kinematics as that of test dummy. Movement of head and pelvis from simulation model follows closely to that of test. Structural deformation of seat back was also observed same as that of test article.

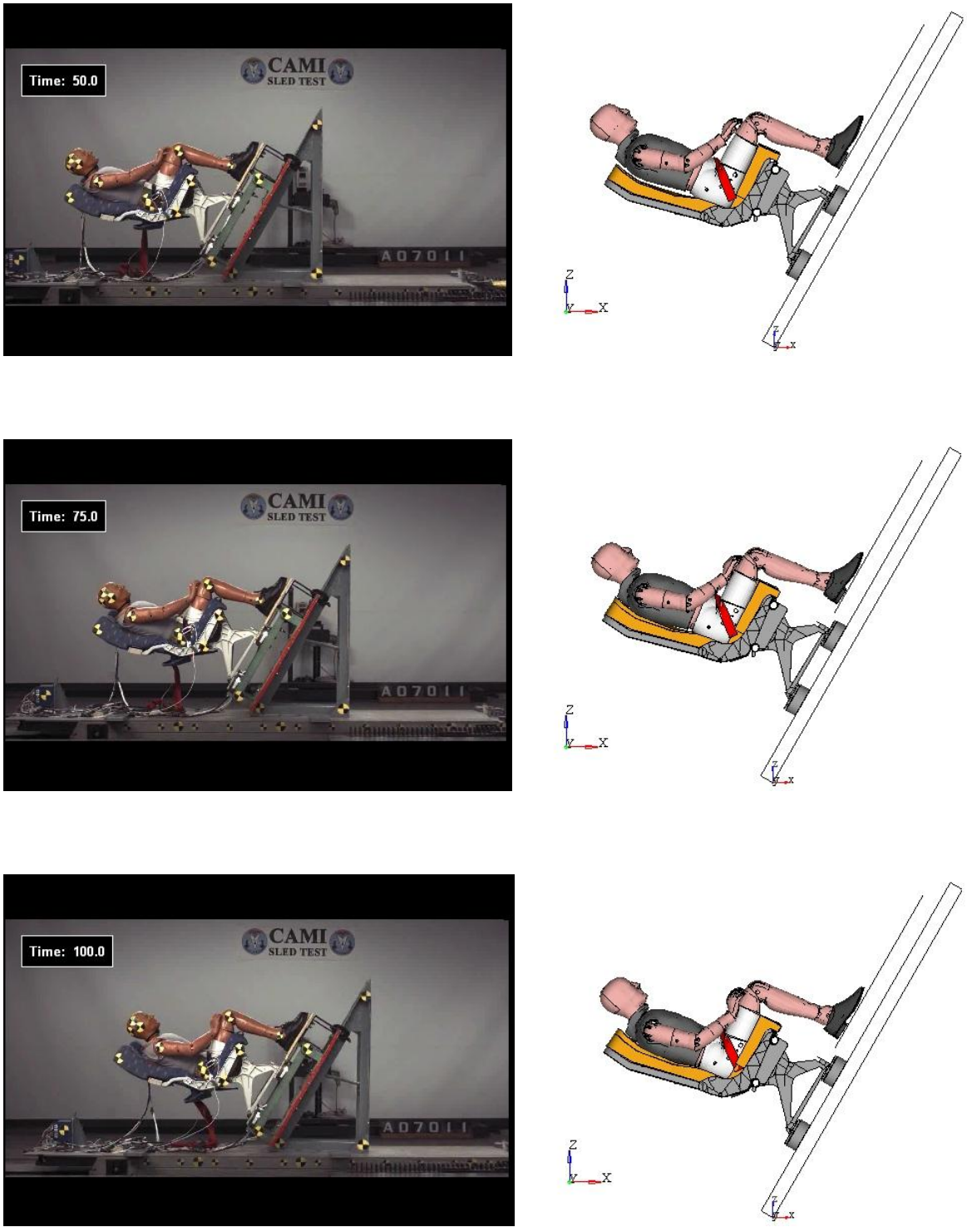

Figure 5-8 Kinematic comparison for test no. 07011

Figure 5-8 Kinematic comparison for test no. 07011 (cont'd)

5.3.2 Validation of the Profiles and Quantitative Comparison

As explained earlier, important channels for test I condition are dummy accelerations and lumbar forces. Table 5-2 shows the comparison results for test no. 07011. Peak values of each channel are also compared and shown in Figure 5-9, Figure 5-10 and Figure 5-11. Since it is a 60 degrees vertical test condition and meant to check the critical lumbar compressive forces, simulation model shows a very good correlation for lumbar compressive force and can be seen in Figure 5-10.

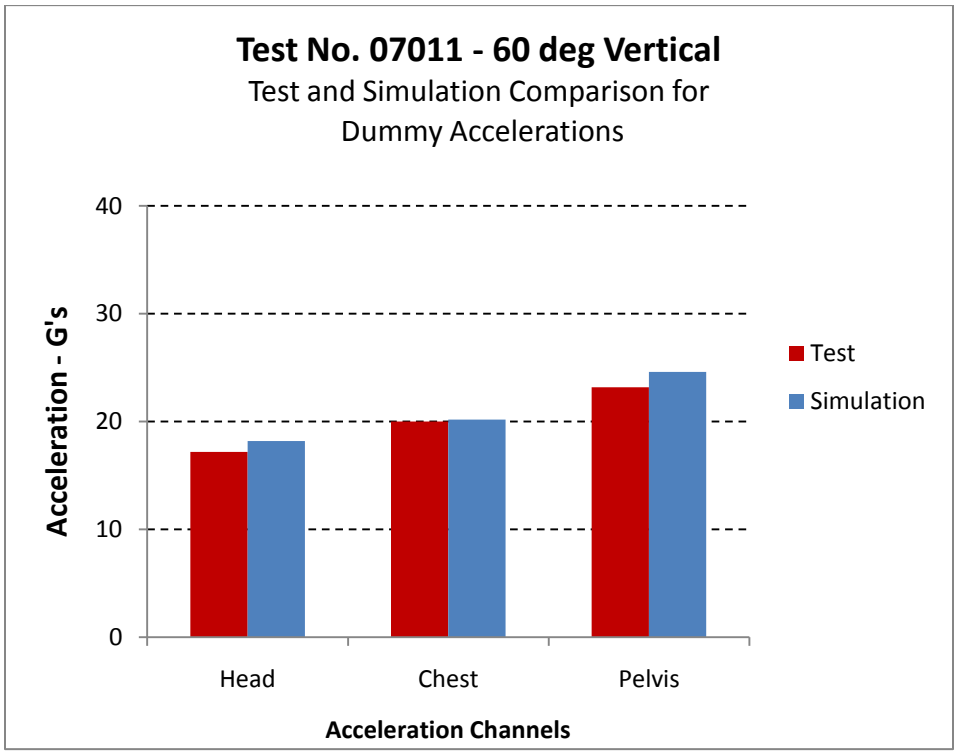

Figure 5-9 Test and simulation comparison for dummy acceleration

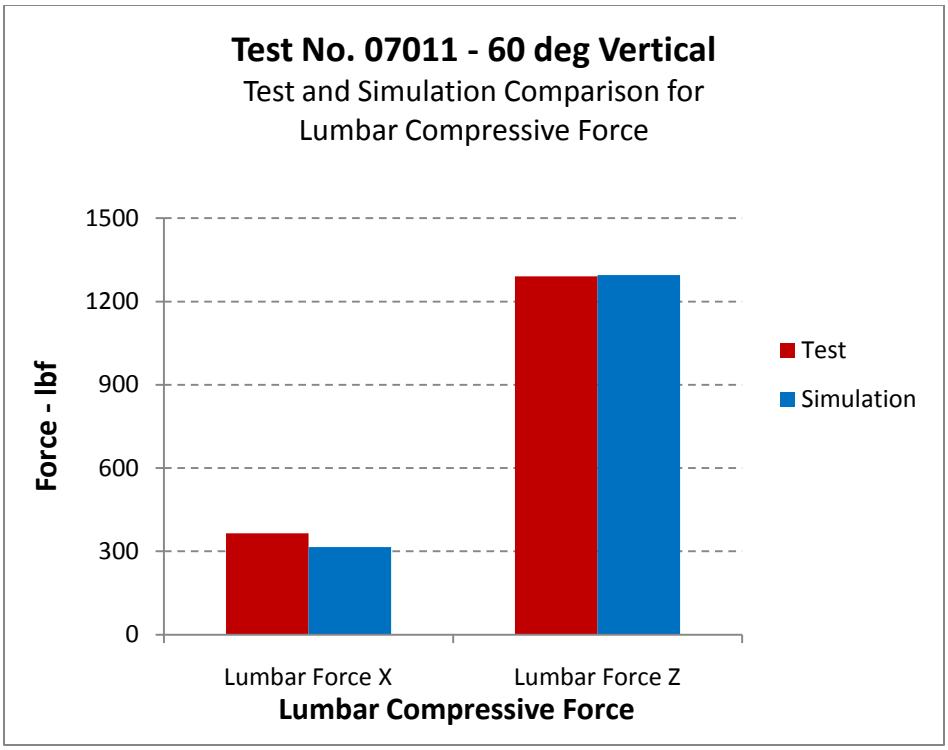

Figure 5-10 Test and simulation comparison for Lumbar force

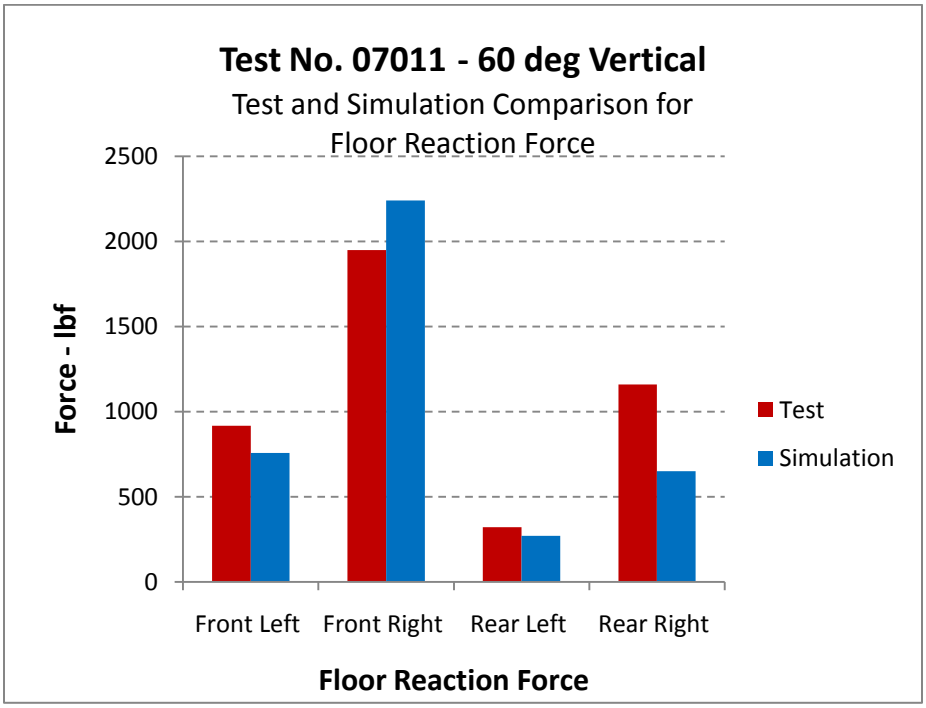

Figure 5-11 Test and simulation comparison for floor reaction force

As for test I condition predominant impact force is along spine/lumbar column of the occupant, making lumbar Z force deciding factor for test pass or fail condition. Simulation model predicts very good correlation with test lumbar Z force and can be seen in the Table 5-2.

Table 5-2 Profile Validation Results for Test No. 07011

Component	**Output channel**	**Mag. Error**	**Shape Error**
Head	Head Acceleration	6%	7%
Torso	Torso Acceleration	0%	11%
Pelvis	Pelvic Acceleration	6%	7%
Lumbar	Lumbar Force X	12%	16%
	Lumbar Force Z	**0%**	**8%**
	Lumbar Moment Y	29%	33%
Lap Belt	Left Lap Belt	34%	37%
	Right Lap Belt	56%	42%
Floor Loads	Front Left Leg	17%	19%
	Front Right Leg	15%	13%
	Rear Left Leg	16%	10%
	Rear Right Leg	43%	39%

The result comparison for belt forces or floor loads shows a higher % differences but this is just because that the original test values for these channels were very small and so even small difference between test and simulation makes the % difference a big value.

CHAPTER 6

PARAMETRIC STUDIES

Table 5-1 and Table 5-2 show the profile comparison results for test and simulation. Simulation results for Test I and II showed correlation of both magnitude and shape error within 10% for critical components. Overall kinematics comparison for both Test I and II condition also showed reasonable correlation and can be seen in Figure 5-3 and Figure 5-8. As per the requirements of AC 20-146 simulation model shows reasonable correlation with test and can be said to be validated for both Test I and II conditions.

AC 21-25A describes the requirements if any of the parts changed or modified on the already certified seats. It requires repeating the certification testing if parts like seat cushion or belt changed on the seat model. But as per AC 20-146 these additional certification testing can be substantiated by the process of "Certification by Analysis", which is very easy, time saving and economical as compared to recertification testing and also acceptable to FAA. The validated simulation model was used to perform two parametric studies. The first study was conducted to replace nylon belt by polyester belt and second was to replace DAX 55 cushion by DAX 26 cushion.

6.1 Belt Replacement

Nylon belt with 20% elongation properties was used on the test article and the loading and unloading characteristics for the belt are shown in Figure 3-30. Since it is a 20% elongation belt it allows a bigger envelop for head displacement. To reduce the head path/displacement this belt was replaced by a polyester belt with 8% elongation properties. The comparison of loading and unloading characteristics of nylon and polyester belt are shown in the following Figure 6-1.

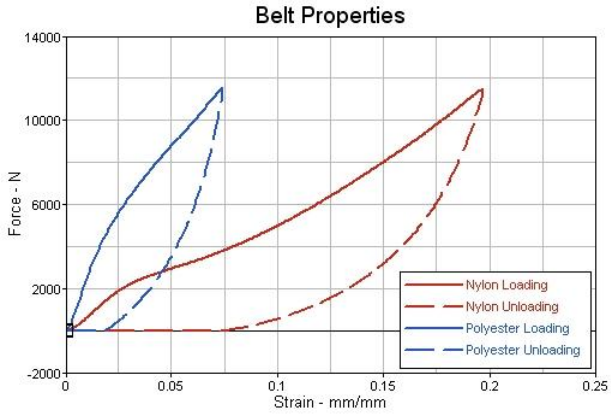

Figure 6-1 Nylon and polyester belt properties

The output results for head path with polyester belt shows a reduced head displacement of 0.7 inch as compared to nylon belt. Head displacement graph can be seen in Figure 6-2.

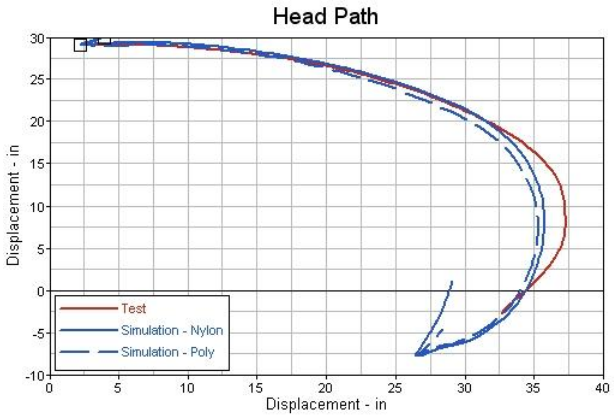

Figure 6-2 Head path comparison of polyester and nylon belt

The output result comparison for belt forces shows the same peak magnitude forces with the use of new 8% elongation belt with different output profile. Comparison for both left and right belt forces is shown in Figure 6-3.

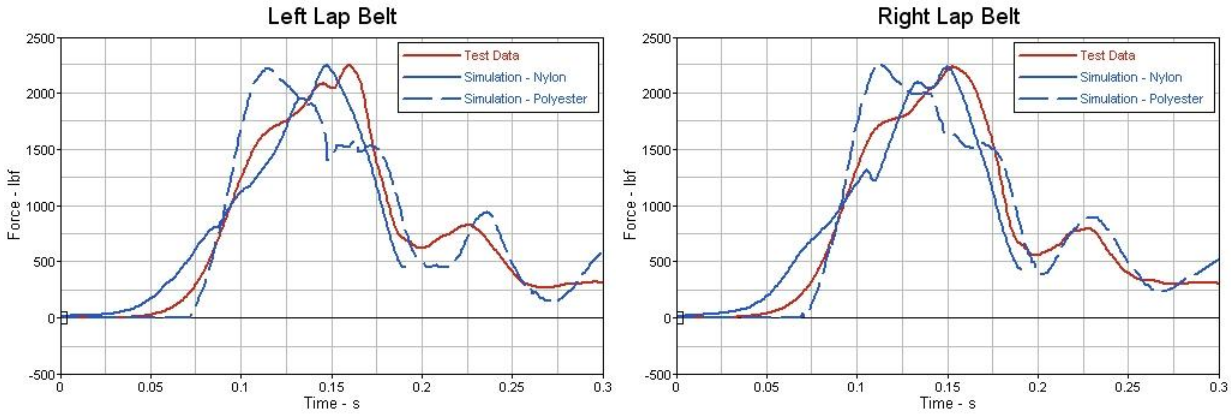

Figure 6-3 Belt forces with polyester and nylon belt

6.2 Cushion Replacement

This parametric study was conducted for Test I condition. Stress strain properties of the DAX 26 cushion that was used on actual testing are shown in Figure 3-28. For this parametric study this DAX 26 cushion was replaced by DAX 55 cushion which is stiffer than the actual cushion. Stress strain properties of both the cushions are shown in the following Figure 6-4.

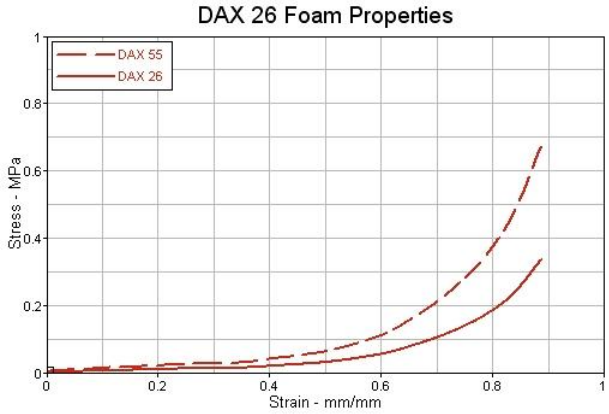

Figure 6-4 Foam stress strain properties

Since the DAX 55 cushion is stiffer than the actual DAX 26 cushion, lumbar compressive force with new DAX 55 cushion shows a less value of 100 lbf than with DAX 26 cushion. The effect of cushion replacement on lumbar compressive force is shown in the Figure 6-5.

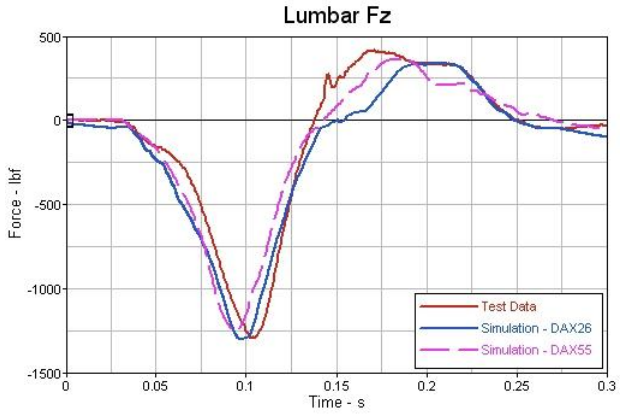

Figure 6-5 Lumbar compressive force

6.3 Dummy Replacement

For this parametric study original FTSS HII 50th % occupant model was replaced with FAA HIII 50th % occupant model. This case study was performed to make sure that FE seat model also gives same results with different type of dummy model and also to check the predictability of FAA HIII 50th % occupant model. This FAA HIII 50th % occupant model was developed by Poltecnico di Milano university from automotive HIII 50th % occupant model. This new FAA HIII occupant model has the same neck structure as that of automotive model and lumbar column is that of aerospace occupant model. This new occupant model was used to simulation Test II condition and results were compared to simulation model with FTSS occupant model. Figure 6-6 shows the comparison of setups with FTSS and FAA occupant models.

Comparison of results for occupant acceleration channels, floor loads and belt forces is shown in Appendix C. Dashed blue line represents results for FAA HIII 50th % occupant model, continuous blue line for FTSS HII 50th % occupant model and red color for test data.

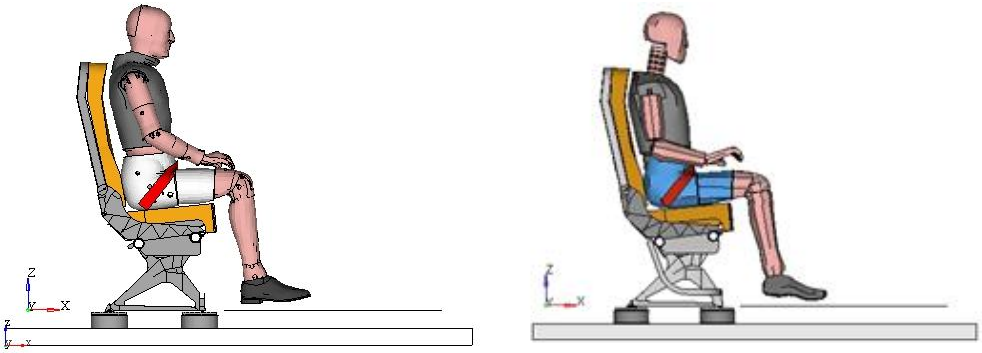

Figure 6-6 Simulation setup comparison

For all the occupant acceleration output channels, both occupant models showed good correlation with test data and comparison can be seen in Table 6-1.

Table 6-1 Comparison of Results With FTSS HII and FAA HIII Occupant Model

Component	**Output channel**	**FTSS HII**		**FAA HIII**	
		Mag. Error	Shape Error	Mag. Error	Shape Error
Head	Res. Acceleration	1%	6%	1%	9%
Torso	Res. Acceleration	9%	14%	4%	15%
Pelvis	Res. Acceleration	18%	10%	20%	12%
Lap Belt	Left Lap Belt	0%	8%	0%	4%
	Right Lap Belt	0%	8%	0%	4%

For head path comparison simulation model with FTSS occupant shows very good correlation with test data as compared to simulation model with FAA HIII occupant model. Simulation model with FTSS occupant shows magnitude error of 5% with that of test and simulation model with FAA HIII occupant model shows magnitude error of 14% with test. And this difference is because of different neck construction of FAA HIII model. Head path comparison is shown in Figure 6-7.

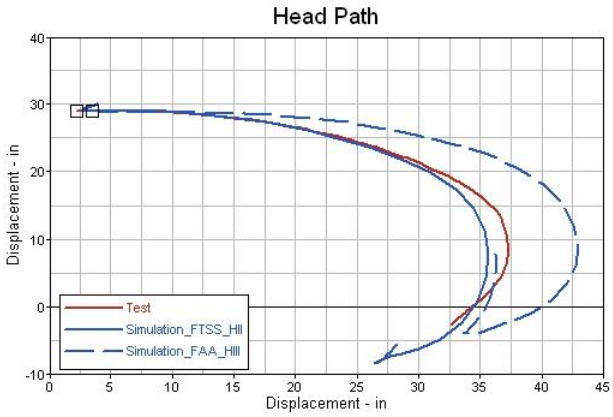

Figure 6-7 Head path comparison

CHAPTER 7

CONCLUSIONS AND RECOMMENDATIONS

Full scale dynamic certification testing of aircraft seats is very expensive and time consuming process. One reliable solution to reduce certification cost is to produce better seat design by predicting the dynamic behavior of seating system, using computer modeling techniques. Advances in computer software and hardware have made it possible to analyze complex systems by numerical simulation. With the availability of low cost, fast computers, it is possible to tackle large crash impact problems. As a result, FEA techniques have become a well-established design tool for predicting dynamic events in the aircraft seat industry.

7.1 Conclusions

Some of the important conclusions drawn from this project are as follows:

- This study developed a very good finite element model of a typical aircraft seat for explicit code LS-DYNA
- FE occupant model FTSS H II 50th% used for this study is a stable model and delivered very good results
- Commonly used meshing procedures are documented in this study
- This study also documented most commonly used material models, element formulations, constraint types and contact models for explicit code LS-DYNA
- Comparison of simulation model results with test data showed a good correlation and established a confidence in finite element methodology
- Computer simulations can really be helpful in product development process

7.2 Future Recommendations

Some recommendations can be suggested after working on this research work

- Some more testing can be done with test II condition to validate the FE model for pitch and roll effects.
- This model can be utilized to study seat installation configurations.
- Simulations with different types of airbags can be performed to reduce dummy injury values.

REFERENCES

LIST OF REFERENCES

[1] Soltis S. J., Nissley W. J., "The development of dynamic performance standards for civil aircrafts seats," Society of Automotive Engineers, 1985.

[2] Anon., "Methodology for seat design and Certification by Analysis," AGATE Report No. C-GEN-341-1, 2006.

[3] Adams A., Lankarani H. M., Nick M., "Development of new crashworthiness evaluation strategy for aircraft seats," American Society of Engineering Education, 2003.

[4] Olschinka C., Schumacher A., "Dynamic Simulation of flight passenger seats," 5th LS-Dyna conference, 2006.

[5] Gabler H., Bowen D., Molnar C., "Modeling of Commuter category aircraft seat," U.S. Department of Transportation, Report No. DOT/FAA/AR-04/34, 2004.

[6] Schoenbeck, A., Schultz M., "Emerging technologies in aircraft crashworthiness," Naval Air Warfare Center, 1999.

[7] Lankarni H., Bhone P., " Finite element modeling strategies for dynamic aircraft seats," Society of Automotive Engineers, 2008.

[8] Anon., "Dynamic evaluation of seat restraint systems and occupant protection on transport airplanes," Federal Aviation Administration, AC No. 25-562, 2006.

[9] Anon., "Methodology for Dynamic Seat Certification by Analysis for Use in Parts 23, 25, 27, and 29 Airplanes and Rotorcraft," U.S. Department of Transportation, AC No. 20-146, 2003.

[10] Anon., "National Aerospace Standards - NAS 809, Specification - Aircraft Seats and Berths," 1991.

[11] Du Bois P. A., "Crashworthiness engineering with LS-DYNA," LS-Dyna Lecture Notes, 2000.

[12] Anon., "Metallic materials properties development and standardization," Office of aviation research, Washington, 2003.

[13] Bala S., "Introduction to LS-DYNA," Livermore Software, 2006.

[14] Hallquist J., “LS-DYNA theory manual,” LSTC, 2006.

[15] Anon., “LS-DYNA Keyword user’s manual,” LSTC, 2007.

[16] Belytschko T., “Finite elements for nonlinear continua and structures,” J. Wiley, 2000.

[17] Olivares G., “Certification by analysis,” JAMS presentation, 2008.

APPENDICES

Appendix A
Test no. 07005 output data channels comparison

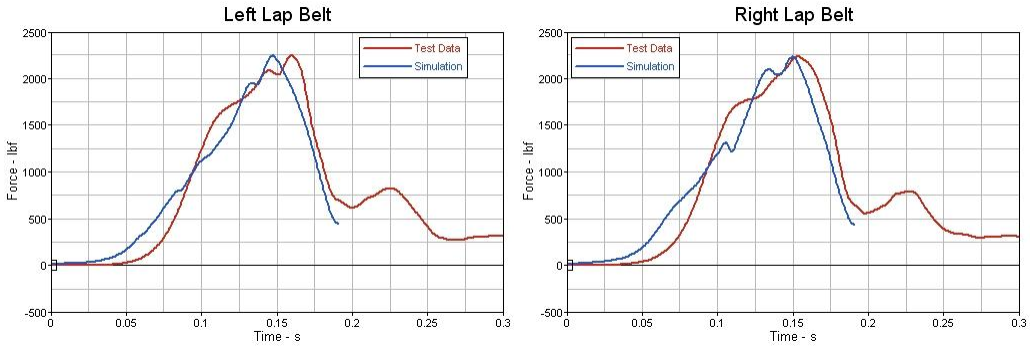

Figure A-1 Lap belt force

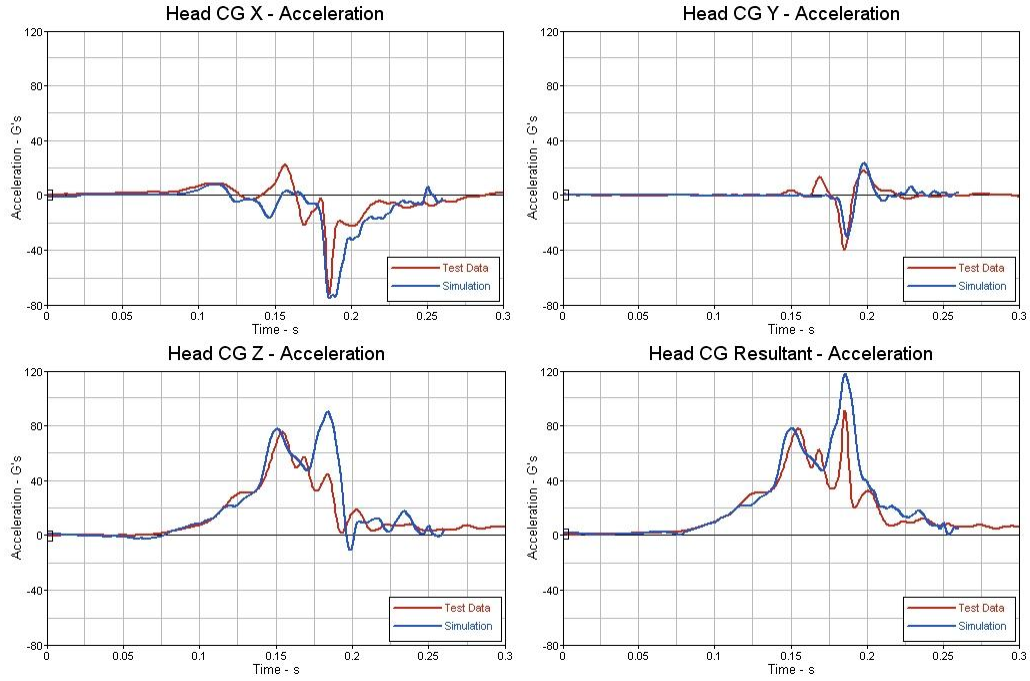

Figure A-2 Head acceleration

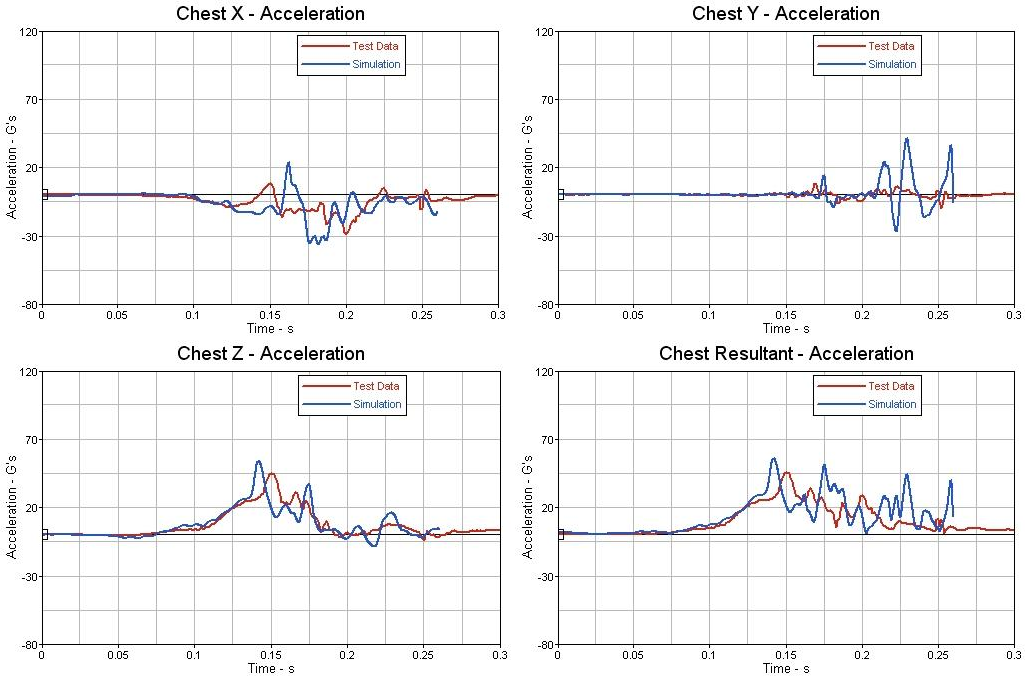

Figure A-3 Chest acceleration

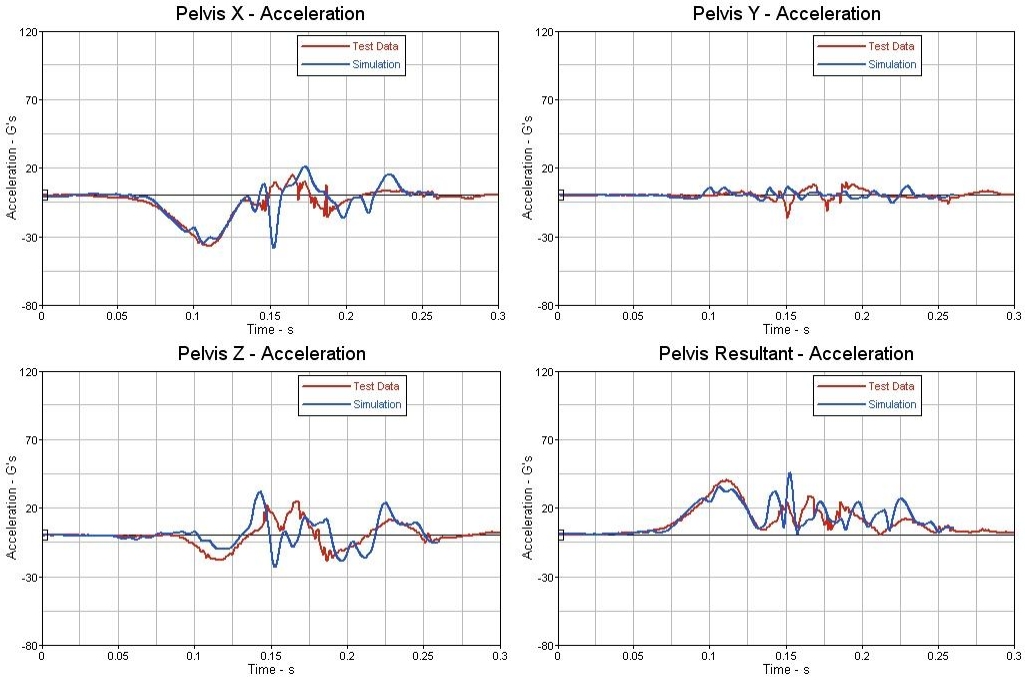

Figure A-4 Pelvis acceleration

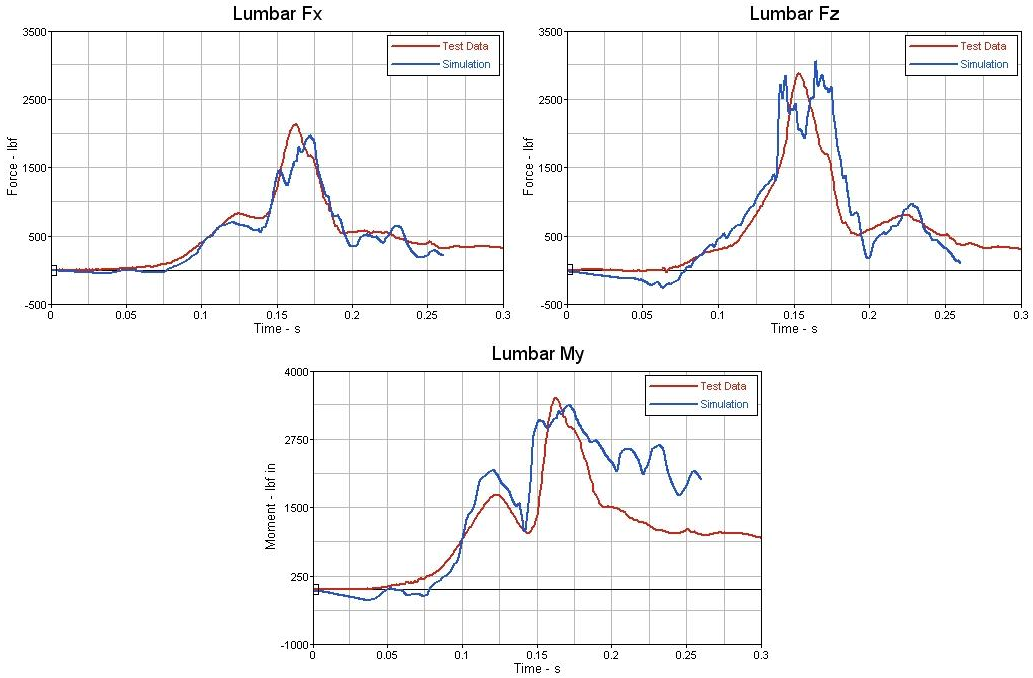

Figure A-5 Lumbar force and moment

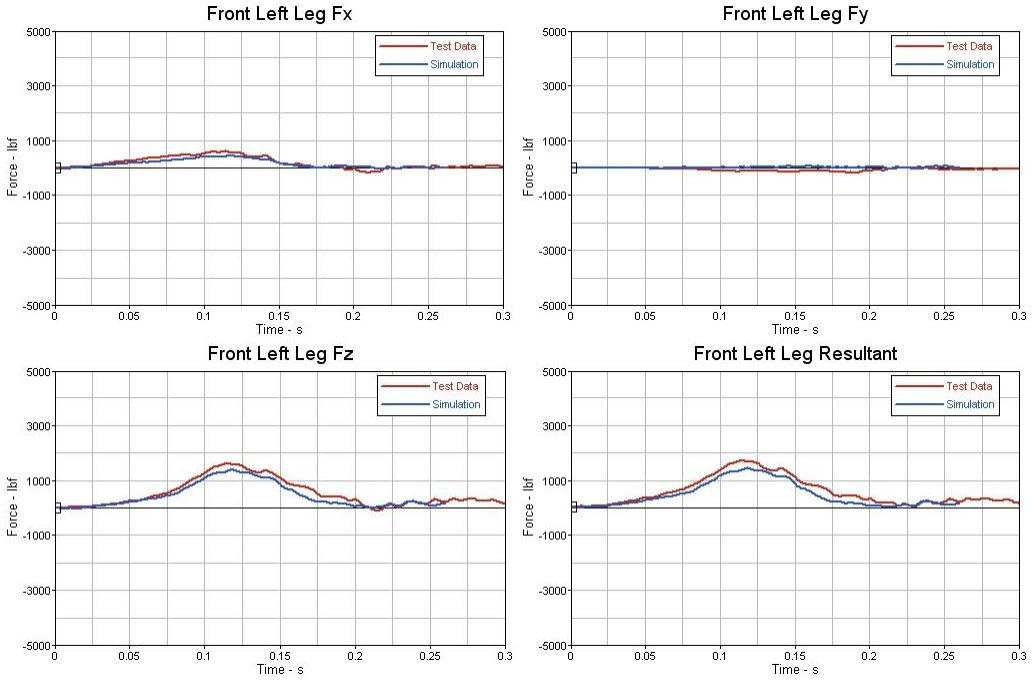

Figure A-6 Floor reaction force

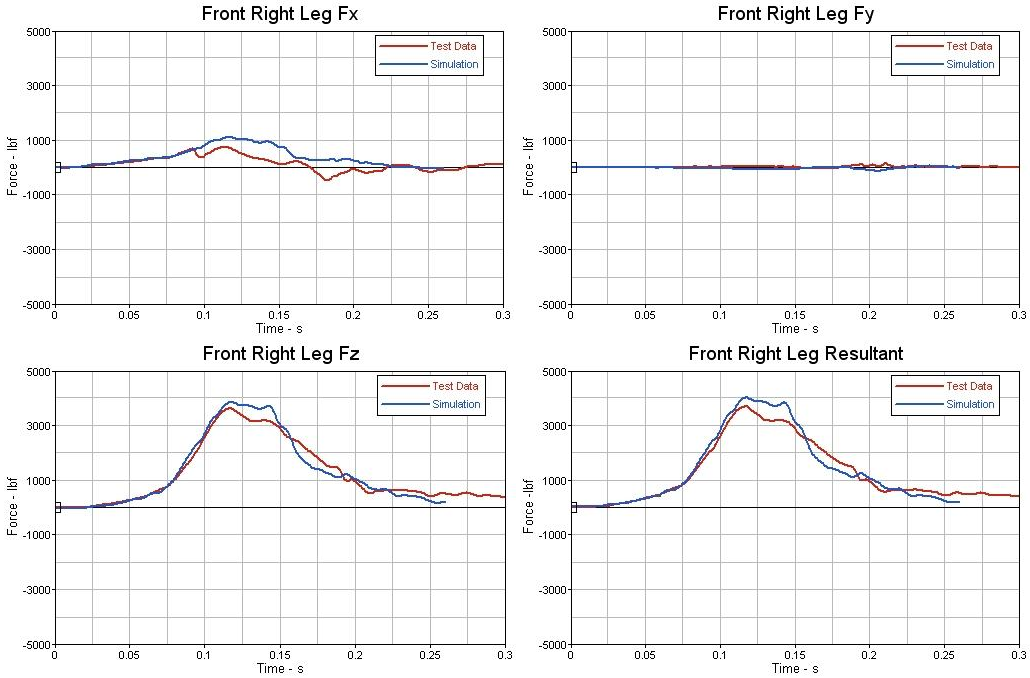

Figure A-7 Floor reaction force

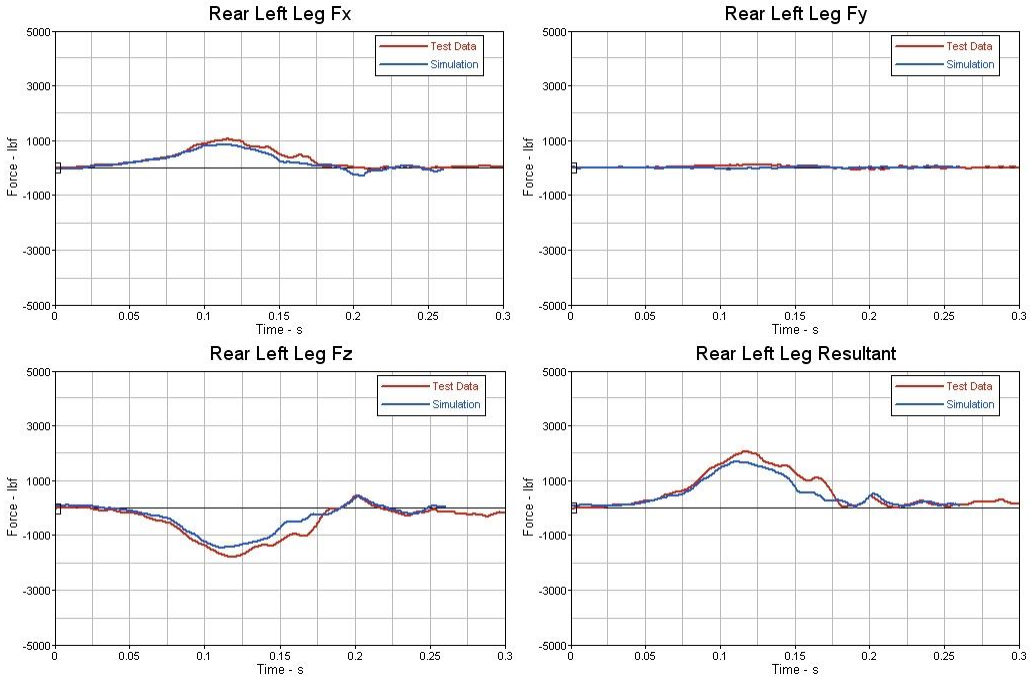

Figure A-8 Floor reaction force

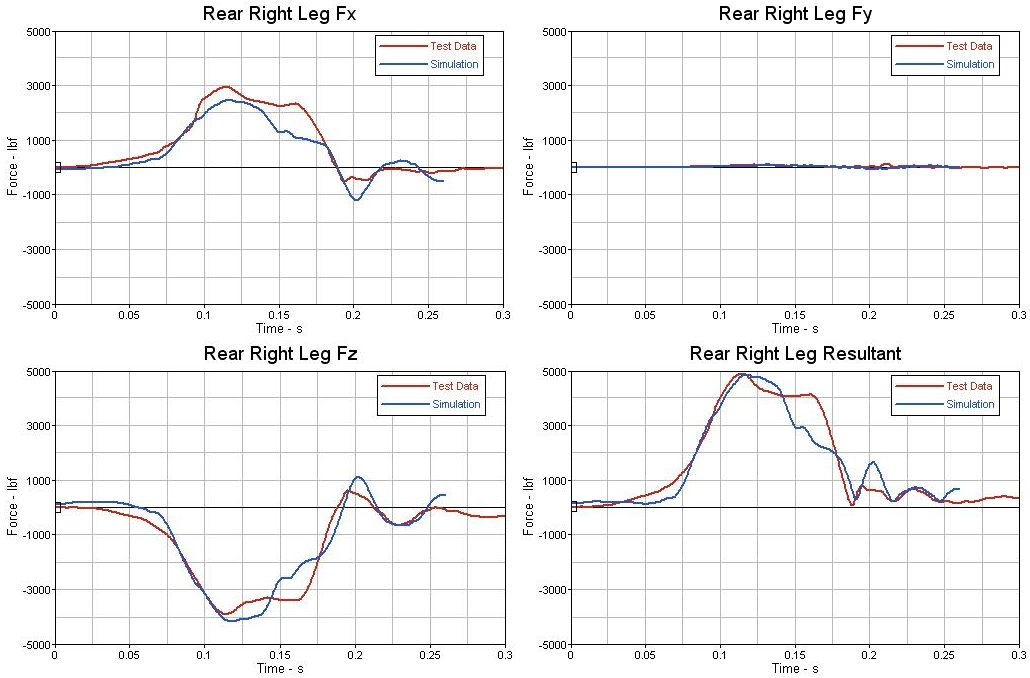

Figure A-9 Floor reaction force

Appendix B
Test no. 07011 output data channels comparison

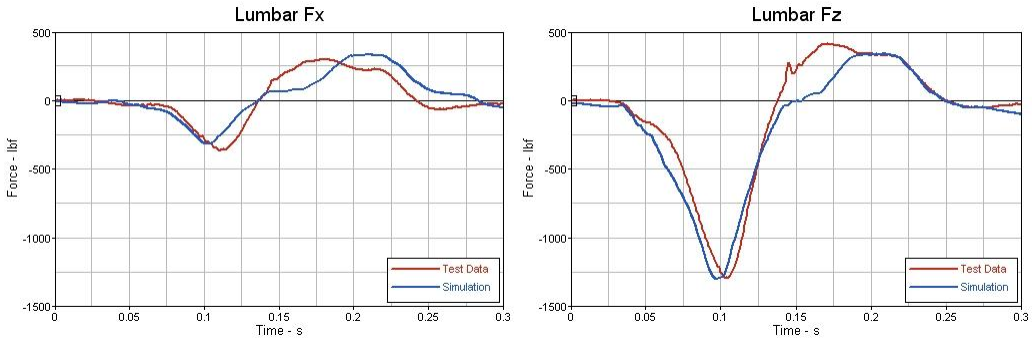

Figure B-1 Lumbar force

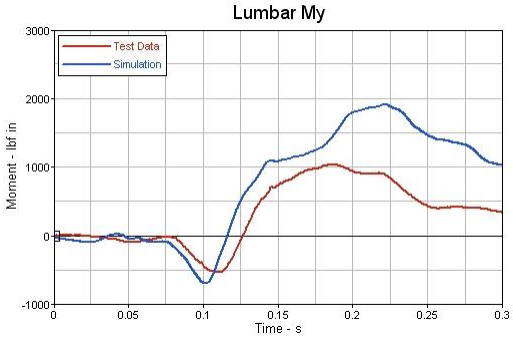

Figure B-2 Lumbar moment

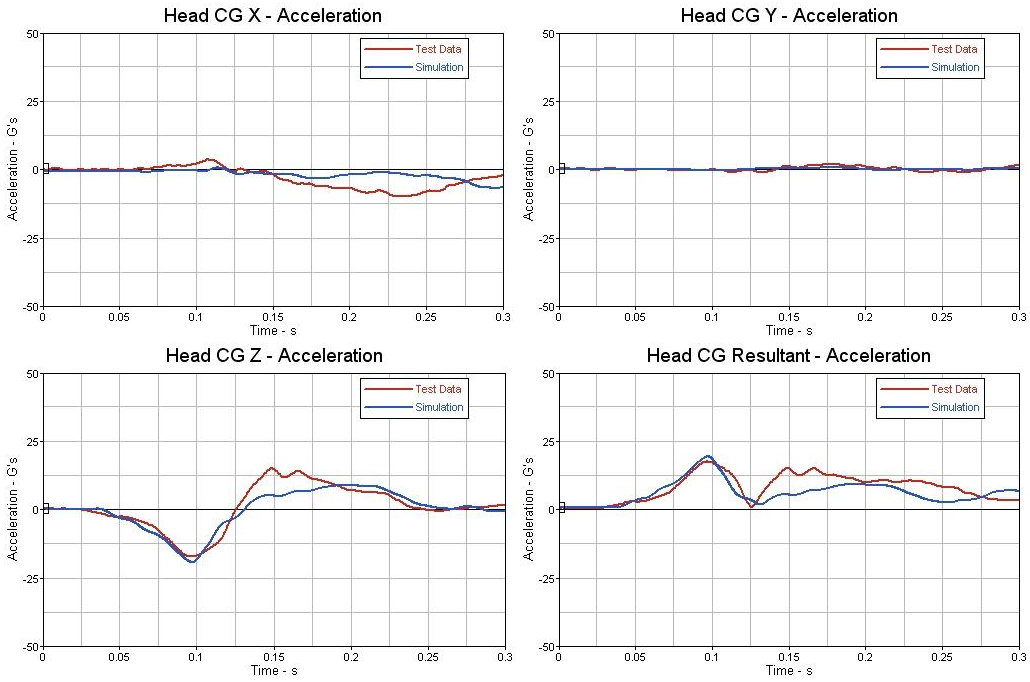

Figure B-3 Head acceleration

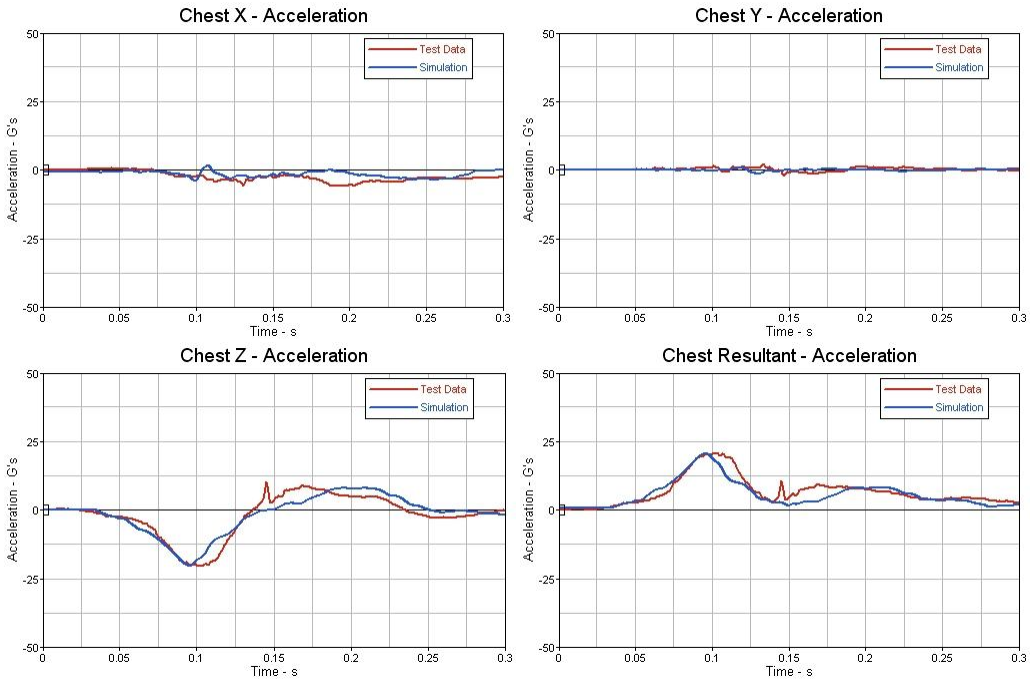

Figure B-4 Chest acceleration

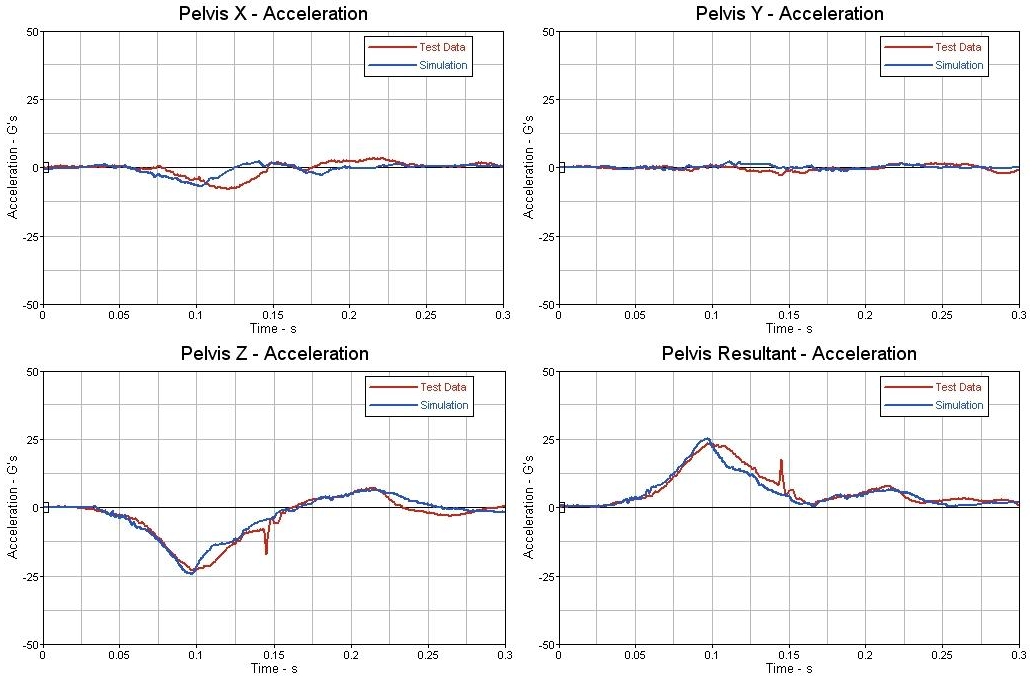

Figure B-5 Pelvis acceleration

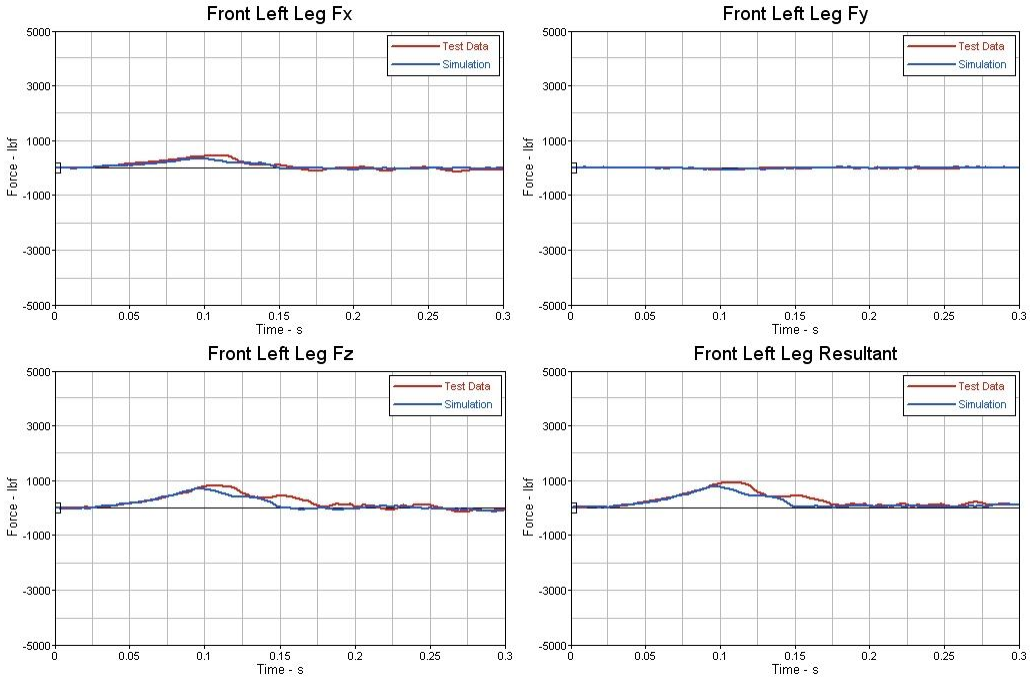

Figure B-6 Floor reaction force

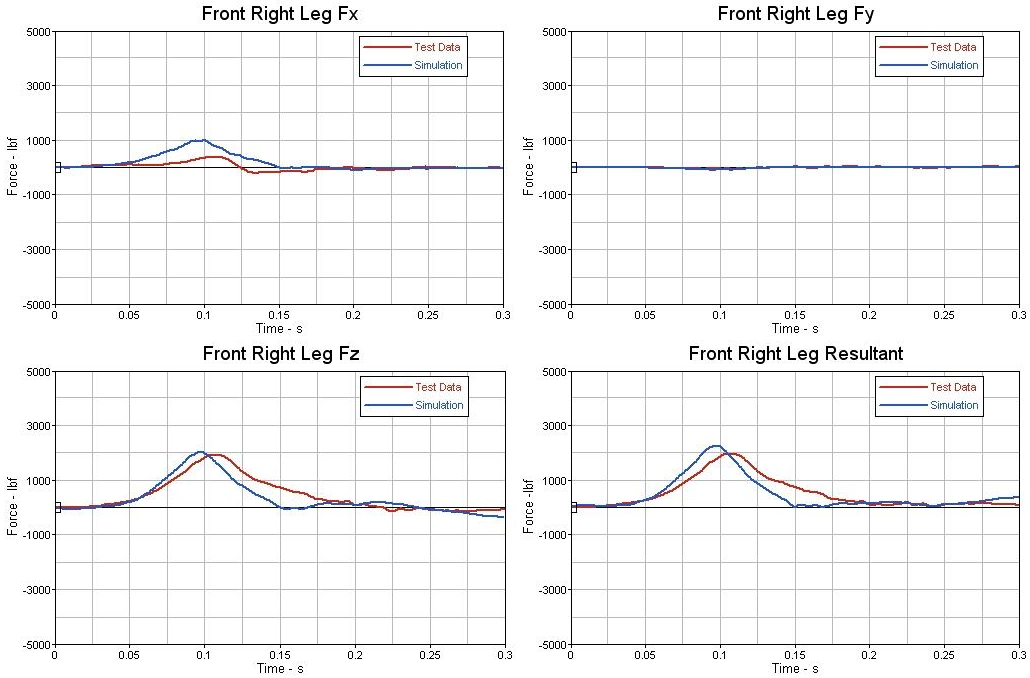

Figure B-7 Floor reaction force

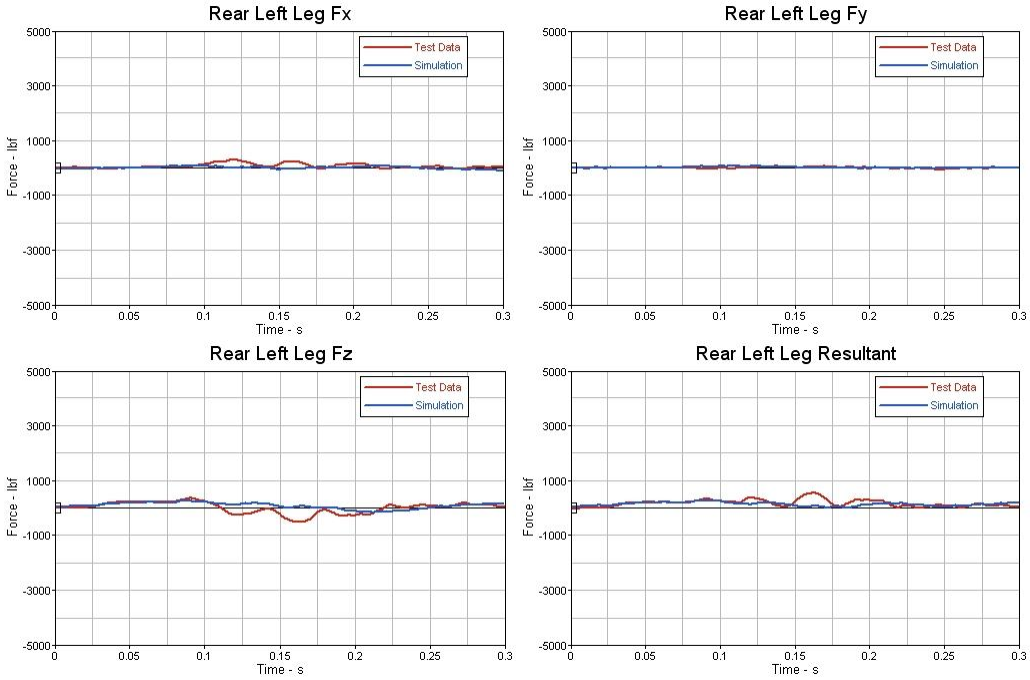

Figure B-8 Floor reaction force

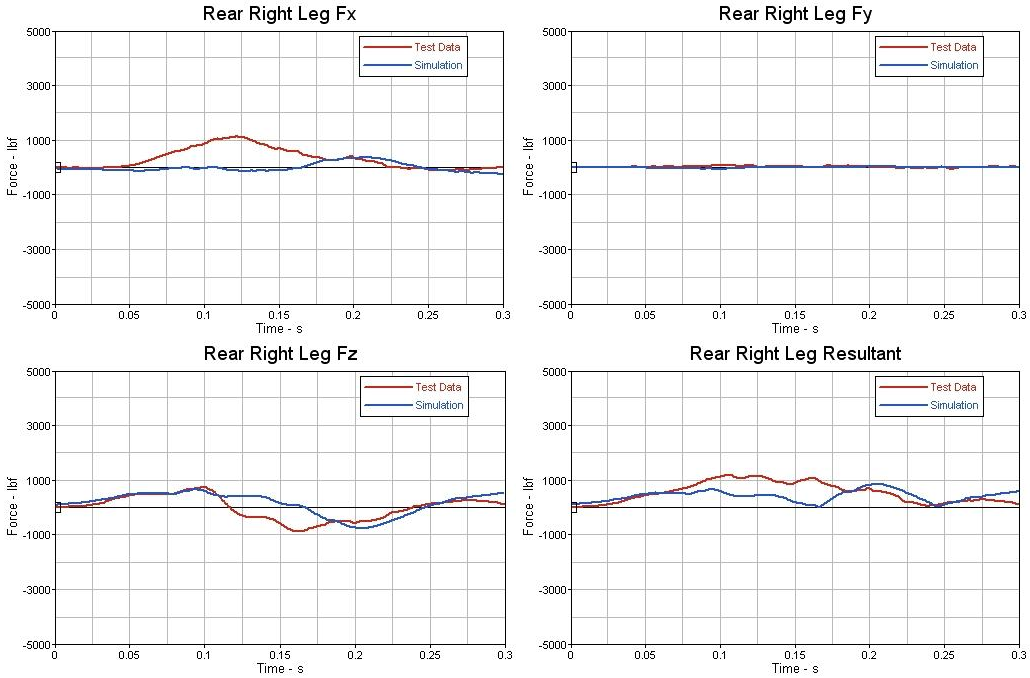

Figure B-9 Floor reaction force

Appendix C
FTSS HII and FAA HIII occupant model output data channels comparison

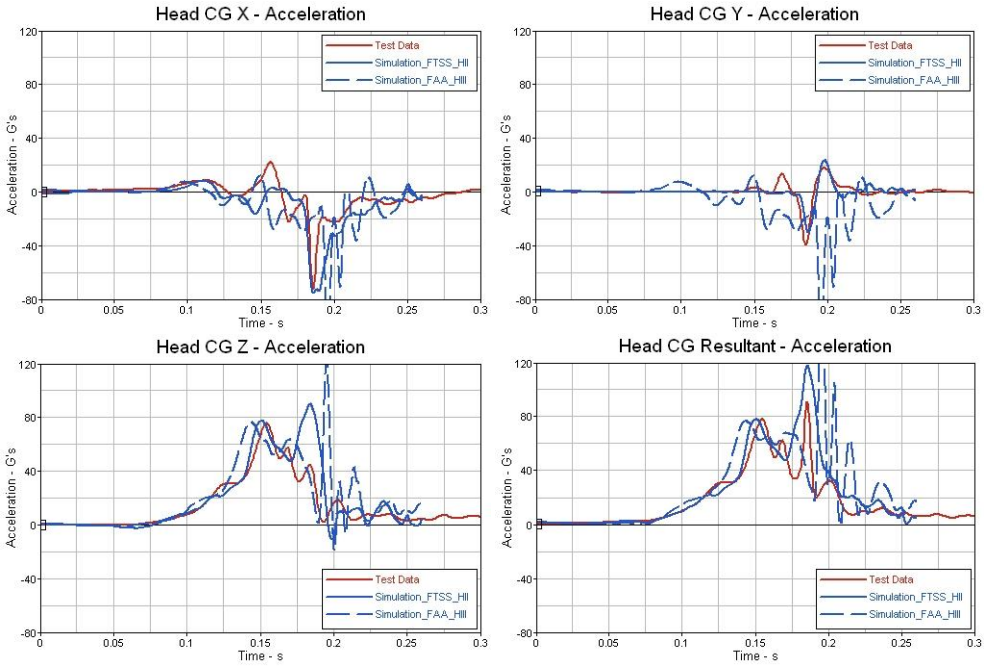

Figure C-1 Head acceleration

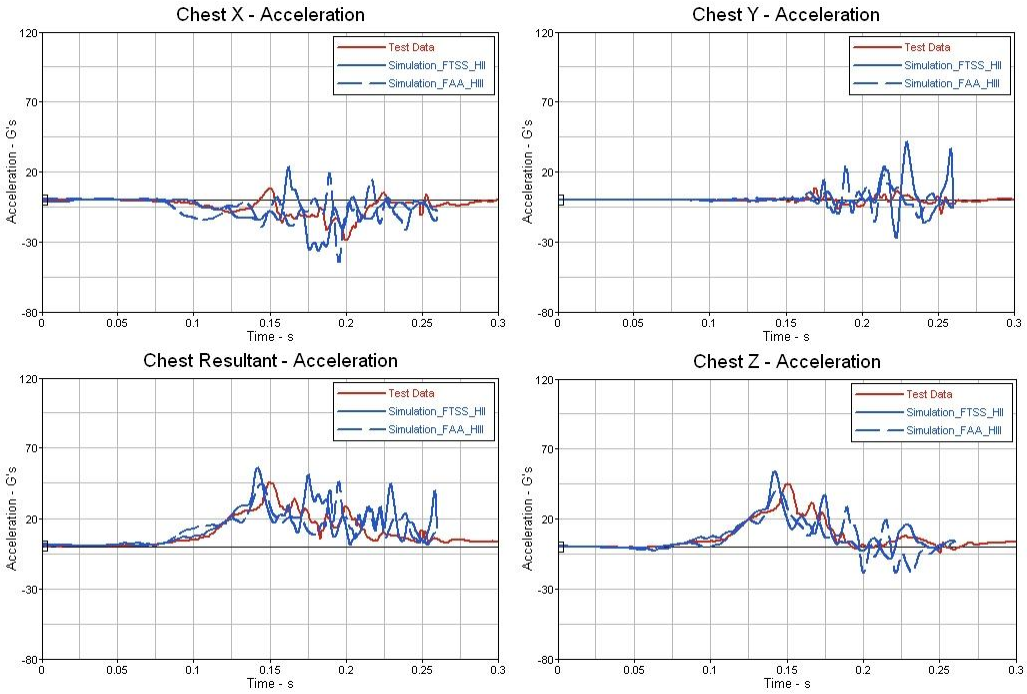

Figure C-2 Chest acceleration

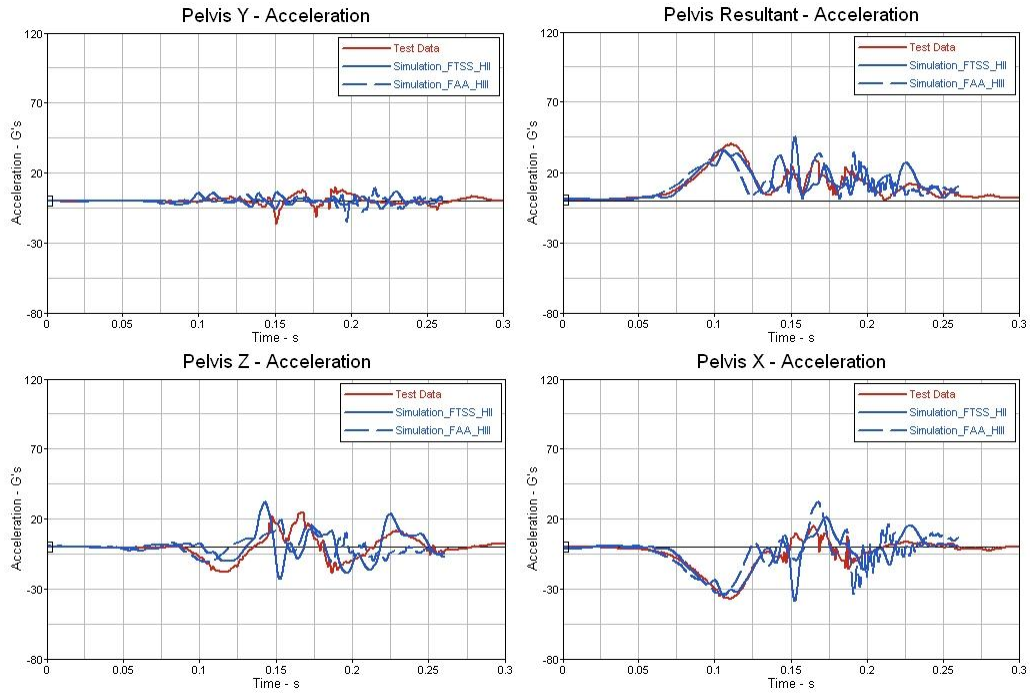

Figure C-3 Pelvis acceleration

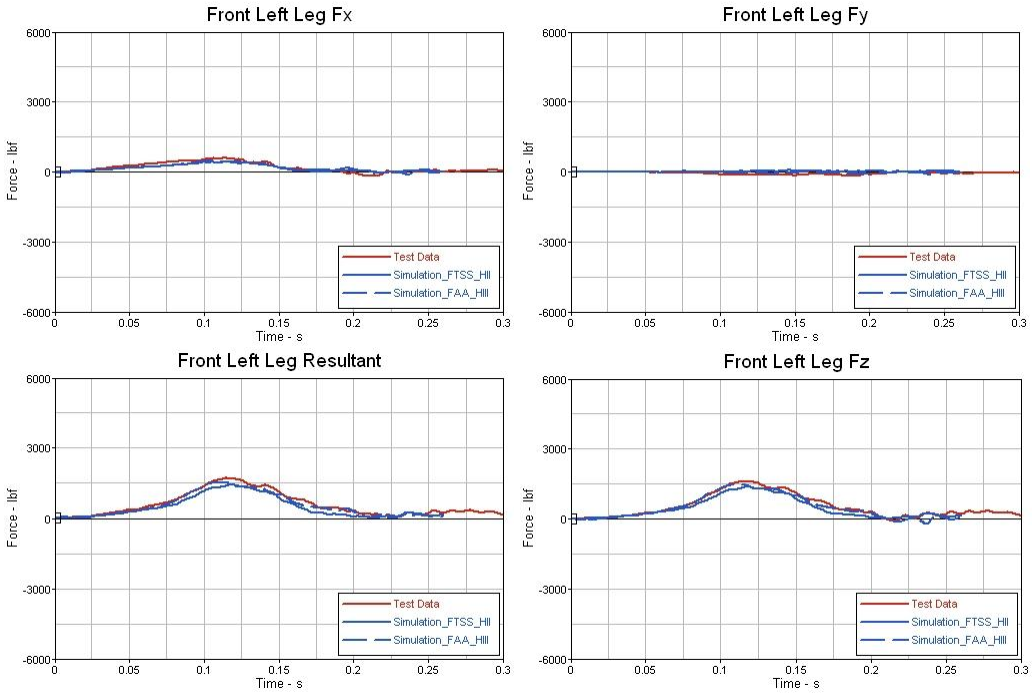

Figure C-4 Floor loads

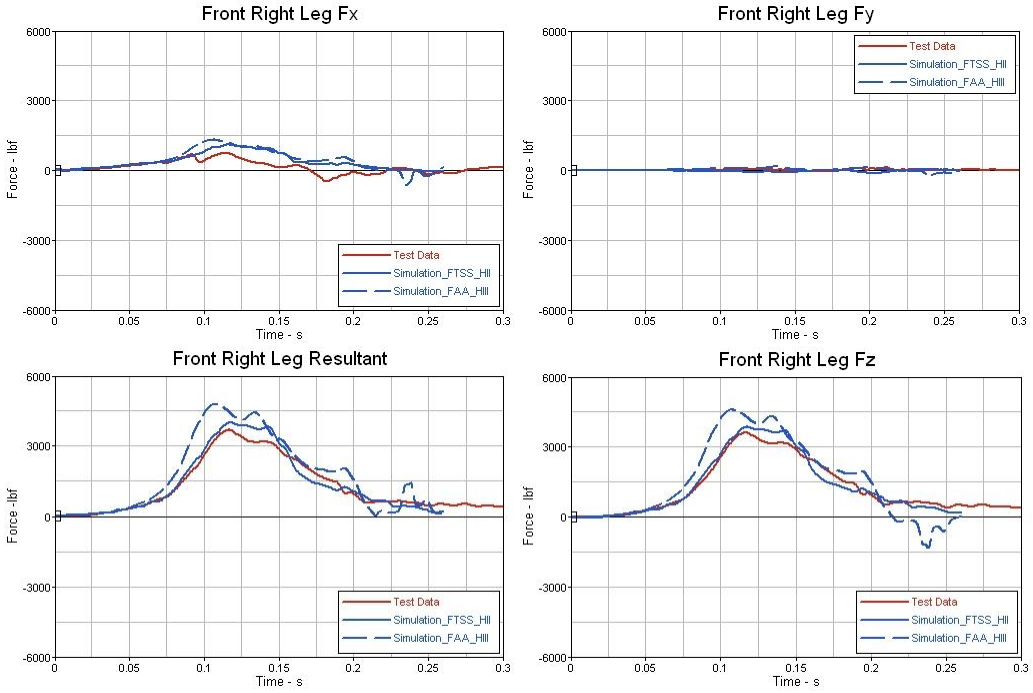

Figure C-5 Floor loads

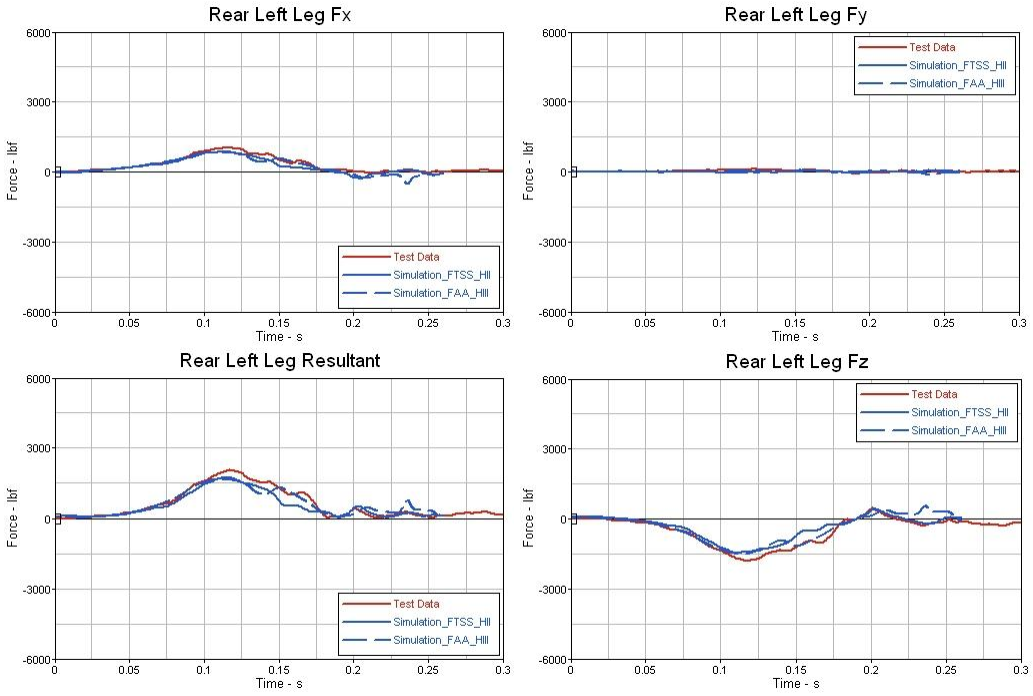

Figure C-6 Floor loads

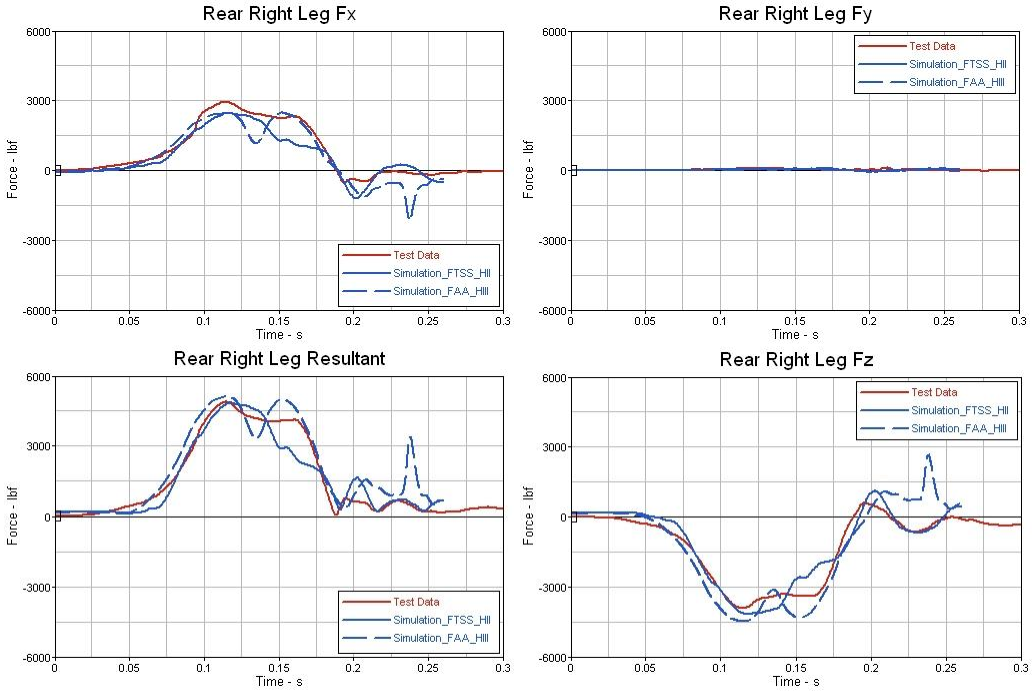

Figure C-7 Floor loads

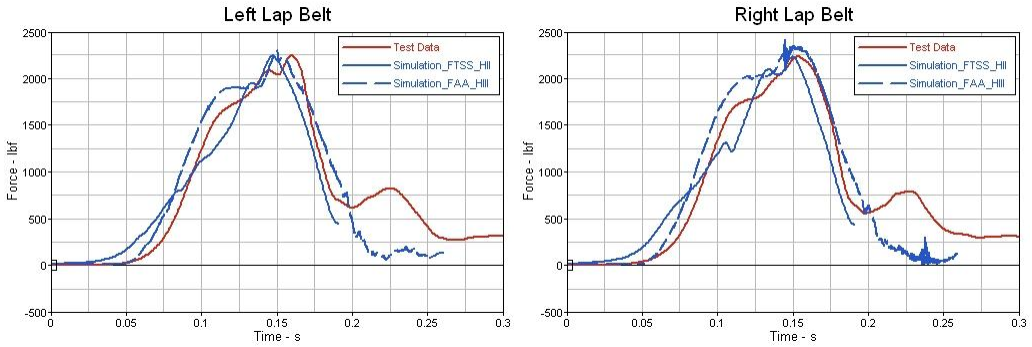

Figure C-8 Belt forces